Integrated analysis of ovarian cancer stem cells-associated lncRNA-miRNA-mRNA network via microarray and Gene Expression Omnibus database

Zheng Li
Shengjing Hospital of China Medical University
Ying Li
Shengjing Hospital of China Medical University
Jinling Bai
Shengjing Hospital of China Medical University
Zhijiao Wang
Shengjing Hospital of China Medical University
Yingying Zhou (20082248@cmu.edu.cn)
Shengjing Hospital of China Medical University

Research Article

Keywords: ovarian cancer stem cells, competing endogenous RNAs, microarray technology, Gene Expression Omnibus (GEO) database

Posted Date: November 4th, 2022

DOI: https://doi.org/10.21203/rs.3.rs-2221089/v1

Abstract

Background

Competing endogenous RNAs (CeRNAs) play an important role in maintenance of ovarian cancer stem cells (OCSCs) characteristics.

Objective

To isolate a new OCSC line and construct a ceRNA network for maintenance of OCSCs characteristics by the cell line and GEO Database.

Methods

We isolated OCSCs from ovarian cancer cell line COC1 by chemotherapy drugs and growth factors. We identified the DEMs, DELs and DEGs between OCSCs and COC1 by microarray and combined them with representative microarray profiles in GEO Database. The ceRNA network was constructed by STRING and Cytoscape. QPCR and western blot were used to verify the expression of several genes that contained in the predicted network.

Results

According to the combination, 28 DEMs were identified at first, and 452 DEGs were obtained combining with the predicted targets of these miRNAs and our mRNA microarray results. Up-regulated DEGs of them were significantly enriched in ‘p53 signaling pathway’, ‘FoxO signaling pathway’, et al, whereas down-regulated DEGs were significantly enriched in ‘Adherens junction’ and ‘Hepatitis C’ pathway. Finally, we obtained OCSCs characteristics related ceRNA network with 10 DEMs, 21 DEGs, and 25 transcripts of 13 DELs. We verified that LINC00665-miR-146a-5p-NRP2 should be one of the pathways of the constructed ceRNA network.

Conclusion

The ceRNA network we constructed may be involved in the stem cell characteristics maintenance of OCSCs and provide directions for further OCSCs research in the future.

1 Introduction

Epithelial ovarian cancer is the most lethal gynecologic malignancy (Aletti et al. 2007), and it’s the fourth most common cause of death from cancer in 40–59 years old women (Siegel et al. 2016). According to

statistics, it's predicted that the increase of incidence should be 22530 in the US in 2019, which accounts for 2.5% of all estimated new tumor cases in women, and 13980 of deaths should occur, accounting for almost 5% of the total of cancer deaths in women (Siegel et al. 2019). The most common therapy is the optimal cytoreductive surgery combined with 6–8 cycles of platinum-based chemotherapy. However, after optimal cytoreductive surgery performance, many patients emerged secondary chemoresistance within one year with chemotherapy, resulting in a recurrence rate of serous ovarian cancer of up to 80% (Lee et al. 2017).

It is reported that many mechanisms play important role in regulation of chemoresistance in ovarian cancer chemotherapy, such as enhancement of repair of DNA damage, reduction of drug accumulation in cells, loss of drug function and inhibition of apoptosis. While cancer stem cells (CSCs) theory gives a new understanding in the development of drug-resistant tumors (Dalerba et al. 2007). CSCs are one unique subpopulation of cells with stem cell proprieties in tumors. This kind of cells remain in a dormant and quiescent state, therefore, exposure to a drug that targets dividing cells at DNA replication and mitosis could not reduce the number of CSCs efficiently (Moore and Lyle 2011; Valent et al. 2012). On the contrary, chemotherapy drugs may increase the ratio of CSCs in tumor tissues because of its inhibitory effect on differentiated tumor cells (Lee et al. 2017). And the expression of drug membrane transporters such as ABCG2 make it difficult for chemotherapy drugs to accumulate in CSCs (Ma et al. 2010). CSCs also can expand the pool of stem cells through symmetric division, or differentiated cancer cells associated with tumor recurrence through asymmetric division, during which stem cells give rise to daughter cells of different fates, proliferative potential, size, or other characteristics (Morrison and Kimble 2006). Sometimes these two kinds of division can be transformed into each other. In summary, CSCs are a kind of 'self-renewing cells within a tumor that can cause the heterogeneous lineages of cancer cells that comprise the tumor' (Clarke et al. 2006). The existence of CSCs means that there is a small population of cells with stem cell properties proliferating slowly and carrying primary resistance to chemotherapy in tumor tissues and these cells can be selected during the period of chemotherapy and pass the drug resistant property to their daughter cells (Sanchez-Garcia et al. 2007). It is also one of the important reasons for ovarian cancer recurrence after chemotherapy. Therefore, CSCs theory, to result in CSCs-dependent cancer recurrence during the treatment of ovarian cancer, is worthy of further study.

There are many methods for CSCs isolation, such as identifying SP cells from ovarian cancer cells by efflux of Hoechst 33342 dye which could be blocked by exposure to verapamil (Szotek et al. 2006), or isolating CSCs by detecting the transmembrane pluripotent marker protein such as CD44+, CD133+ (Alvero et al. 2009; Lee et al. 2016) and CD117+ (Zhang et al. 2008) at the use of flow cytometry. CD133 has been used as a means of detecting CSCs in many malignancies, including epithelial ovarian cancer (EOC)(Schmohl and Vallera 2016). In ovarian cancer, CD133 + cancer cells have stronger tumorigenicity than CD133- cancer cells and are more likely to develop chemoresistance (Kwon and Shin 2011). While CD117, which is also known as c-Kit, is commonly used to identify CSCs among EOC cells(Yang et al. 2017). CD117 is tyrosine kinase type receptor, which is involved in cell differentiation, proliferation, apoptosis, migration, and other biological processes. It has been suggested that human ovarian cancer cells with CD 117 + phenotype had properties like those of CSCs, such as self-renewing, differentiation,

high tumorigenicity and chemoresistance (Luo et al. 2011). In some studies, CSCs were obtained by recognizing CD117+/CD133 + cells. The CD117+/CD133 + CSCs subpopulation of HO8910, which was the human EOC cell line, were identified to be more likely to develop resistance to conventional chemotherapy agents including cisplatin, doxorubicin, and mitoxantrone(Yan et al. 2014). Li Ma, et al had obtained CD117+/CD133 + cells identified stem cell properties with cisplatin and paclitaxel selection and under the stem cell culture condition from serous ovarian cancer cell line SKOV3 (Ma et al. 2010). According to their protocol, we selected CD117+/CD133 + cells from serous ovarian cancer cell line COC1 for our further study.

Competitive endogenous RNA (ceRNA) theory indicates that specific RNAs can prevent miRNAs from bind to target genes, impair miRNAs activity, and thus up-regulate miRNA target genes expression. In addition to being involved in the occurrence and development of tumors, this regulation mechanism plays an important role in the stem characteristics maintenance of CSCs. For example, there was an estrogen-mediated E2F6 ceRNA network which epigenetically and competitively inhibited miR-193a activity, up-regulated OCSCs marker c-Kit expression, and promoted ovarian cancer stemness and tumorigenesis(Cheng et al. 2019a). The latest study also found that as an oncogenic lncRNA in cervical cancer, LINC00337 affected the expression of KLF5 and maintained the CSC-like properties by down-regulating miR-145(Han et al. 2020). At present, there are many studies on the involvement of lncRNAs as ceRNAs in the occurrence and development of ovarian cancer(Braga et al. 2020), but fewer in the cancer stem cell characteristics regulation. There even has been no report on the constructed ceRNAs network that were associated with stemness maintenance in ovarian cancer. Herein, we analyzed the differentially expressed miRNAs, lncRNAs and mRNAs by microarray, and obtained the key differentially expressed miRNAs (DEMs) by combining with representative microarray profiles in GEO Database. The predicted target genes of these DEMs (identified by PicTar (Chen and Rajewsky 2006), Targetscan (Agarwal et al. 2015), DIANA (Sethupathy et al. 2006) and starbase (Li et al. 2014)) and the differentially expressed mRNAs (DEGs) of our microarray and GEO database were combined to identify key DEGs that were differentially expressed and had the same trend in all these datasets. STRING database (search tool for the retrieval of interacting genes/proteins) is used to construct a protein-protein interaction network (PPI network). Cytoscape can be used to analyze PPI, protein-DNA, and miRNA-mRNA interactions. It supports multiple data input formats, foreign data import, and can also directly construct network diagrams by the editor module of the software itself. Hence, PPI of these DEGs were constructed by STRING (Snel et al. 2000) and Cytoscape (Shannon et al. 2003) to find hub genes in OCSCs. Differentially expressed lncRNAs (DELs) that may interact with these DEMs were obtained by combining the predicted results of lncBase (Paraskevopoulou et al. 2013) and starbase with our lncRNA microarray results. Finally, we obtained the ceRNAs network constructed by miRNA, lncRNA and mRNA in OCSCs. MiR-146a-5p and LINC00665 of this network were selected for partial validation. Through bioinformatics methods, we constructed ceRNAs network that might be involved in the stem characteristics maintenance of OCSCs. The study of OCSCs can help to reveal the CSCs related way in which ovarian cancer develops chemoresistance and provide a theoretical basis for the research on reducing or reversing chemoresistance during the treatment of ovarian cancer.

2 Materials And Methods

2.1 Cell culture and drug screening

Human serous epithelial ovarian carcinoma cell line COC1 was bought from China Center for Type Culture Collection (CCTCC). The cells were seeded in 6-well plate and cultured in the 37 ℃, 5% CO2 incubator, feeding with RPMI-1640 medium (Gibco, 31800-014, US) supplement with 10% fetal bovine serum (Hyclone, SH30084.03, US). Centrifuged and then changed the medium after 24 h culture. The cells were feeded with the same medium above until they grew to 80% confluence. After treated with 40 μmol/L cisplatin and 10 μmol/L paclitaxel(Ma et al. 2010), the cells were cultured for another 5 days (Teramura et al. 2008). Then passed the cells after centrifuging and maintained them under stem cell conditions, which was composed of RPMI-1640 medium (Gibco, 31800-014, US), 5μg/ml recombinant human insulin (Solarbio, 11061-68-0, China), 10ng/ml recombinant human epithelial growth factor (EGF, Sino Biological Inc, 10605-HNAE, China), 10 ng/ml basic fibroblast growth factor (bFGF, Sino Biological Inc, 10014-HNAE, China) and 12 ng/ml leukemia inhibitory factor (LIF, Cloud-Clone Corp, RPA085Hu01, US) (Ma et al. 2010). Changed the medium every other day by centrifuging at 1000 rpm for 5 min, and then collected the cells after 6 days for further gene expression and protein detection.

2.2 Sphere formation assay

The floating sphere cells were dissociated by incubation with 0.25% trypsin–EDTA for 1–2 min at 37℃. Next, 100 cells per well were plated in 96-well culture dishes in 200 μl of growth medium; 25 μl of medium per well was added every 2 days. The number of dissociated spherical cells for each well was evaluated after 7 days of culture.

2.3 Flow cytometric analysis

The dissociated cells were centrifuged at 1000 rpm for 5 min and then yielded. Wash the cells two times by phosphate buffered solution (PBS, Doublehelix, P10033, China) and collected the cells at 1000 rpm for 5 min. After centrifugation, the supernatant was discarded. The 1 × 106 cells were resuspended with 100 μl PBS supplement with anti-CD133 (eBioscience, 12-1339-41, APC, US), anti-CD117 (eBioscience, 11-1178-41, APC, US) and control antibody (mouse non-specific IgG for CD133 and CD117, 70-CMG105-10 and 70-CMG104-10, MultiSciences, China), respectively. The percentage of CD133 and CD117 positive cells (CD133+/CD117 + cells) was performed by flow cytometric analysis after incubated in dark.

2.4 Regulation of LINC00665 expression

The cells were cultured in a 5% CO2 incubator at 37℃. Transfection can be carried out when the cell density was 70%. LINC00665 coding DNA sequence (CDS) region was amplified by polymerase chain reaction (PCR) and cloned. The sequence was ligated with pcDNA3.1 (+) and then transformed and the positive clones were selected and over-expression of LINC00665 was confirmed by sequencing analysis and PCR. The resulting DNA oligo annealed shRNA template and linearized pSico vector (Promega, US) were ligated to construct an expression vector with LINC00665 suppression. The vector was transformed

into competent bacteria. The positive clones were selected, and LINC00665 suppression was confirmed by sequencing analysis. (Supplementary Table 1)

2.5 RNA extraction and real-time quantitative PCR (qPCR)

Total RNA was extracted according to the protocol of total RNA kit (BioTeke, RP1201, China). The concentration of the RNA extracted was calculated, then 1 μg of total RNA was added into 19 μl reverse transcription mixture for reverse transcription polymerase chain reaction (RT-PCR) according to the protocol of PrimeScript™ RT reagent Kit (Perfect Real Time) (Takara, RR037Q, China). The gene expression was detected according to the protocol of SYBR Green (Solarbio, SY1020, China) method by using the ExicyclerTM 96 fluorescent quantitative machine (BIONEER, Korea). The primers sequences are showed in Table 1. The reaction cycle is: 94 ℃ for 10 min, 94 ℃ for 10 s, 60 ℃ for 20 s, 72 ℃ for 30 s, repeated 40 cycles, 72 ℃ for 2 min and 30 s, 40 ℃ for 5 min and 30 s, 60 ℃ to 94 ℃, 1.0 ℃ per 1 s, 25 ℃ for 1 min. The data were analyzed by 2−ΔΔCT method and the CT (threshold cycle) value means the number of cycles after which a signal of each sample could be detected. And β-actin was used as internal reference control for normalization.

Table 1
Primes of qPCR.

F represents 3 ' upstream primers and R represents 5' downstream primers. The reaction conditions have been listed in the part of Materials & Methods.

Name	F	R
miR-146a-5p	TGAGAACTGAATTCCATGGGTT	GTGCAGGGTCCGAGGTATTC
LINC00665	GGTGCAAAGTGGGAAGTGTG	AGTCCGGTGGACGGATGAGAA
miR-183-5p	GCGGCTATGGCACTGGTAGAA	GTGCAGGGTCCGAGGTATTC
miR-96-5p	TTTGGCACTAGCACATTTTTGCT	GTGCAGGGTCCGAGGTATTC
NRP2	GAATGGCTACTATGTCAAATCC	GAGGGCGATACCTGAGTG
β-actin	GGCACCCAGCACAATGAA	CGGACTCGTCATACTCCTGCT
U6	GCTTCGGCAGCACATATACT	GTGCAGGGTCCGAGGTATTC

2.6 Western blot

Cell lysis buffer (Beyotime, P0013, China) was used to lyse COC1 and spheroid cells at 4 ℃ for 5 min. The debris was removed by centrifugation at 12000 rpm, 4 ℃ for 10 min and the supernatant protein extract was analyzed for western blot. The quantitative determination of protein was made according to the manufacturer's instructions (BIOTEK, ELX-800, US). The protein sample diluted by 5×Loading Buffer and PBS was boiled in boiling water for 5 min. The volume of each sample was 20 μl containing 40 μg protein. SDS-polyacrylamide gel electrophoresis (SDS-PAGE) was performed after protein loaded at 80 V

for 2.5 h. Then the protein was transferred to a polyvinylidene fluoride (PVDF, Millipore, IPVH00010, US) membrane by electroblotting. The transferred PVDF was put into the 5% (w/v) milk diluted by TBST buffer supplemented with 0.05% Tween 20 for 1 h to block nonspecific reaction. The membrane was incubated with rabbit anti-human OCT4 antibody (1:500, Abcam, ab18976, UK), rabbit anti-human SOX2 antibody (1:500, Abcam, ab97959, UK), rabbit anti-human NANOG antibody (1:500, Abcam, ab80892, UK), rabbit anti-human ALDH1 antibody (1:500, Abclonal, A0157, China), rabbit anti-human LGR5 antibody (1:500, Abclonal, A12327, China) and rabbit anti-human NRP2 antibody (1:1000, Affinity, DF7032, China) overnight at 4 ℃, followed by incubated with goat anti-rabbit secondary antibody (1:5000, Abcam, ab7090, UK) or goat anti-rabbit secondary antibody (1:5000, wanleibio, WLA023, China). ECL western blot detection reagents (Pierce) were used for protein imaging according to the manufacturer's instructions by Gel-Pro-Analyzer (Beijing Liuyi, WD-9413B, China). β-actin (wanleibio, WL01845, China) was used as an internal reference.

2.7 Immunofluorescence staining

The cells were plated on an eight-well chamber slide for 24–48 h. The cells were fixed with 4% PFA/PBS (paraformaldehyde/phosphate buffer solution) for 10 min at room temperature and then washed with PBS thrice and treated with 0.5% Triton X-100in PBS for 5 min. The slides were then washed twice with 0.01% Tween in Trisbuffered Saline (TBS-T). After blocking with 1% bovine serum albumin (BSA) in TBST, the slides were incubated overnight at 4℃ with primary antibody for rabbit monoclonal antibody Lgr5 (1:100, Novus, MAB8078-SP, USA), rabbit polyclonal antibody ALDH1 (1:300, Wanleibio, WL02762, China), rabbit monoclonal antibody SOX2 (1:100, Abclonal, A0561, China), rabbit monoclonal antibody OCT4 (1:100, Affinity, AF0226, China) and rabbit monoclonal antibody Nanog (1:100, Affinity, AF5388, China).After washing with TBST for 10 min, thrice at room temperature, the slides were incubated with secondary antibody for 1 h at room temperature: FITC conjugated goat anti-rabbit IgG (1:100, Abcam, ab6717 UK) and Cy3 conjugated goat anti-mouse IgG (1:200, Invitrogen, A-21424, USA). The slides were washed with TBST for 10 min thrice and then counterstained with DAPI (0.5 mg/mL DAPI/TBST) for 10 min. The slides were mounted with anti-fluorescence quenching agent (Solarbio, S2100, China) and photographed with BX53 (OLYMPUS, Japan). The deletion of the primary antibody from the blocking buffer was used as a negative control.

2.8 Bioinformatics research methods

Agilent Human miRNA, Release 21.0 (8*60K, Design ID:070156) was used in this study for analysis of DEMs. Agilent Human lncRNA V5 (4*180K, Design ID:076500) was used in this study for analysis of DGLs and DEGs. Experiments were performed according to the instruction of the manufacturer. Differentially expressed genes, lncRNAs or miRNAs were identified through fold change. The threshold set for up- and down-regulated genes was a fold change ≥ 2.0. We identified the DEMs by combining with representative microarray profiles in GEO Database (GSE107155-SKOV3 and -Kuramochi), according to the results of GEO2R analysis. PicTar, Targetscan, DIANA and Starbase were used to predict the target genes of these DEMs. The results of each group were analyzed to find the common genes as the DEMs

prediction target genes dataset in OCSCs. The obtained target genes were further combined with our microarray results to identify a set of miRNA target DEGs. At the same time, we identifed the common DEGs by combining our microarray profiles with GEO Database (GSE80373 and GSE28799). The obtained DEGs were further combined with the miRNA target DEGs to identify common DEGs in both sets. Differentially expressed lncRNAs (DELs) that may interact with DEMs were obtained by lncBase (Paraskevopoulou et al. 2013) and starbase, and combined with our lncRNA microarray results. (Supplementary Table 2)

GO and KEGG analyses were performed for each group of DEGs (Huang da et al. 2009a; Huang da et al. 2009b). GO includes three parts: Biological Process (BP), Cellular Component (CC) and Molecular Function (MF). The number of DEGs included in each GO entry was counted, and the significance of enrichment of DEGs in each GO entry was calculated by statistical test. $P < 0.05$ indicated that the DEGs were enriched in this GO entry. Pathway analysis of DEGs was carried out using KEGG database and statistical test was used to calculate the significance of enrichment of DEGs in each pathway entry. $P < 0.05$ indicated that the DEGs were enriched in this pathway. The relationship between the expression and survival probability of key genes was analyzed by Km Curve (Nagy et al. 2018). Finally, we analysed the ceRNA network constructed by miRNA, lncRNA and mRNA in OCSCs by STRING and Cytoscape.

We downloaded a standardized Pan-Cancer data set from the UCSC (https://xenabrowser.net/) database: TCGA TARGET GTEx (PANCAN, N = 19131, G = 60499). Further, we extracted the expression data of LINC00665 and NRP2 in each sample. Sample groups are as follows: Solid Tissue Normal, Primary Solid Tumor, Primary Tumor, Normal Tissue, Primary Blood Derived Cancer-Bone Marrow, Primary Blood Derived Cancer-Peripheral Blood. We performed a Log2(FPKM + 1) transformation on each of the expressed values. P-adjusted values were used for reporting TCGA data. Finally, we eliminated the cancers with a single sample size less than 3 and obtained the expression data of LINC00665 in 34 cancers and their corresponding benign tumors and tissues, and expression data of NRP2 in 34 cancers and their corresponding benign tumors and tissues. We used R software (Version 3.6.4) to calculate the difference in expression between normal and tumor samples in each tumor. (Supplementary Table 6, 7)

2.9 Statistical analysis

Data analysis was performed using SPSS 16.0 (IBM) statistical software. Numerical data were presented as mean ± standard deviation (SD), and categorical data were presented as percentage. To compare the mean values of two related groups, homogeneity of variance test and unpaired samples t-test were performed. The Bonferroni test was used for pairwise comparisons of three data sets. Unpaired Wilcoxon Rank Sum and Signed Rank Tests were used for significance analysis of differences. $P < 0.05$ was considered statistically significant.

3 Results

3.1 Preparation of CD117+/CD133 + ovarian cancer cells and detection of stem cell characteristics

Cells treated with cisplatin (40 μmol/L) and paclitaxel (10 μmol/L) were cultured under stem cell conditions for 6 days to form cell spheres. (Fig. 1A) Western blot analysis and immunofluorescence staining of sphere cells showed that the expression of SOX2, OCT4 and NANOG were higher than those of COC1, and the expression of ALDH1 and LGR5, which were OCSCs-specific stem cell markers, were also increased. (Fig. 1B, Supplementary Fig. 1) Flow cytometry detection showed that the percentage of CD117+/CD133 + cells in sphere was significantly higher (78.5%) than that in COC1 (27.8%). (Fig. 1C, $p = 0.0133$) Cell cycle detection showed that the percentage of M stage of spherical cells was significantly higher (89.2–96.8%) than that in COC1 (2.7%). (Fig. 1D) Therefore, CD117+/CD133 + cells were ovarian cancer stem cell-like cells (OCSCs).

3.2 MiRNA-target regulatory network was established by combining miRNA microarray and GEO datasets results

The results of miRNA microarray were combined with GSE107155-SKOV3 and GSE107155-Kuramochi to find common DEMs. 28 DEMs were identified. (Fig. 2A) In our miRNA microarray results, 15 of them up-regulated and 13 down-regulated in OCSCs. In GSE107155-SKOV3 dataset, 24 of them showed increased expression, while only 4 DEMs showed decreased expression. While the results of GSE107155-Kuramochi dataset suggested that all these 28 DEMs were up-regulated. According to our miRNA microarray results, miR-1268a was the most significantly up-regulated miRNA and miR-324-5p was the most significantly down-regulated one. MiR-630 was the most significantly upregulated miRNA in GSE107155-SKOV3 and -Kuramochi datasets. MiR-221-3p was the most significantly downregulated one in GSE107155 SKOV3 dataset. (Supplementary Table 3)

After analysis by PicTar, Targetscan, DIANA and Starbase, potential target genes of these DEMs were combined with the mRNA microarray results to find common DEGs. Finally, 285 up-regulated and 167 down-regulated DEGs were identified. (Table 2) These DEGs were the predicted target genes for 24 of the 28 DEMs.

Table 2

Potential differentially expressed target genes (DEGs) of the 28 differentially expressed miRNAs (DEMs), which obtained by combining mRNA microarray results with PicTar, Targetscan, DIANA and Starbase results. 285 up-regulated and 167 down-regulated DEGs were identified. Only the top 25 DEGs with the greatest expression difference were listed in each group. All the DEGs listed in the table showed significant differences, $P < 0.05$. And the fold change of each gene was more than 2.

Up-regulated DEGs		Down-regulated DEGs	
Gene name	Fold change	Gene name	Fold change
CHRD	24.64	*LONRF1*	-3443.92
BHLHE41	11.39	*TLE4*	-373.14
PRDM1	10.33	*PRR9*	-9.36
YPEL5	10.05	*SLC2A14*	-9.32
TSC22D3	8.86	*PRKCDBP*	-8.67
NLGN2	7.32	*NAV3*	-8.01
NR1D1	7.27	*MAT2A*	-7.93
CAPS	6.91	*TET2*	-7.45
RFFL	6.75	*SYNCRIP*	-6.44
RASA4	6.50	*PSEN2*	-6.39
PCDH18	6.38	*MAT2A*	-6.27
NLN	6.35	*PCDHGC4*	-6.17
DIO2	6.30	*PPP2R2C*	-6.15
SMIM14	6.07	*HOMEZ*	-6.00
AK7	6.02	*MRPS25*	-5.68
PLD6	5.87	*USP6NL*	-5.60
CLMN	5.80	*EGFR*	-5.58
ADAM10	5.76	*ZSWIM5*	-5.57
NF1	5.54	*CLDN2*	-5.51
BBX	5.54	*KLHL6*	-5.21
EIF4A2	5.48	*UBA5*	-4.89
PIGV	5.44	*AP1S3*	-4.82

Up-regulated DEGs		Down-regulated DEGs	
NRP2	5.36	*UBTF*	-4.64
TMEM154	5.29	*NLGN1*	-4.46
KIAA0430	5.26	*EPHB3*	-4.36

KEGG pathway analysis found that these genes were significantly enriched in ‘Salivary secretion’, ‘Ras signaling pathway’, ‘p53 signaling pathway’ and ‘AMPK signaling pathway’, et al. The tumor-related pathways in which 285 up-regulated genes were significantly enriched included ‘p53 signaling pathway’, ‘FoxO signaling pathway’ and ‘MicroRNAs in cancer’, et al. There were 2 KEGG pathways which the 176 down-expression genes significantly riched in, such as ‘Adherens junction’ and ‘Hepatitis C’, but for the other pathways, ‘Notch signaling pathway’ and ‘Endometrial cancer’, the P values were > 0.05. (Fig. 2B)

GO functional enrichment analysis was performed on these 452 DEGs. It was indicated that these genes were significantly enriched in ‘regulation of GTPase activity’ (BP, GO: 0043087), ‘cytosol’ (CC, GO: 0005829) and ‘protein binding’ (MF, GO: 0005515). 285 up-regulated genes were significantly enriched in ‘cell migration’ (BP, GO: 0016477), ‘nucleus’ (CC, GO: 0005634) and ‘ATP binding’ (MF, GO: 0005524), et al. (Fig. 2C) 167 down-regulated genes were significantly enriched in ‘positive regulation of transcription from RNA polymerase II promoter’ (BP, GO: 0045944), ‘nucleoplasm’ (CC, GO: 0005654) and ‘protein binding’ (MF, GO: 0005515), et al. (Fig. 2D)

Using STRING and cytoHubba, we had obtained the top 10 key genes of these DEGs, ranked by Maximal Clique Centrality (MCC) degree. (Table 3, Fig. 3B) According to MCODE analysis, there were 16 clusters, among which the most significant cluster included 11 nodes and 55 edges. The top 10 key genes were all included in this cluster. UNKL, GNAQ, NMD3, CPD, YPEL5, GAPVD1, VIM, EIF4EBP2, RND3, CALB2, STX16, NHLRC3, TNFRSF21 and OAS2 were seed genes of these clusters. (Fig. 3A, C)

Table 3

The top 10 key genes of PPI network of the target DEGs, ranked by Maximal Clique Centrality (MCC) degree. The top 10 key genes were ranked by Maximal Clique Centrality (MCC) degree. The highest score was FBXO32. RNF14, UBE2H, UBA5, FBXL16 and LONRF1 had equal scores and were ranked the third. RNF115, Hector D1 and TRIM4 had equal ratings and were all ranked the eighth.

Rank	Name	Fold change	Score
1	*FBXO32*	2.44	3628810
2	*UBE2L6*	2.03	3628806
3	*RNF14*	2.17	3628802
3	*UBE2H*	3.39	3628802
3	*UBA5*	-4.89	3628802
3	*FBXL16*	2.52	3628802
3	*LONRF1*	-3443.92	3628802
8	*RNF115*	-2.24	3628801
8	*HECTD1*	2.07	3628801
8	*TRIM4*	2.63	3628801

3.3 MiRNA-lncRNA regulatory network was established by combining miRNA, lncRNA microarray, lncBase and starbase results

LncBase and Starbase were applied to predict the lncRNA transcripts that could bind to the 24 DEMs mentioned above. Combined with our lncRNA Microarray result, we found that 29 transcripts of 17 lncRNA could bind to 14 of the 24 DEMs. (Supplementary Table 4) 22 transcripts were up-regulated, and 7 transcripts were down-regulated in OCSCs compared with common ovarian cancer cells according to our lncRNA microarray analysis.

3.4 Functional enrichment analysis, establishment of protein-protein interactions (PPI) network and and identification of hub genes in OCSCs

Microarray analysis of DEGs was combined with GSE80373 and GSE28799 datasets. As a result, 105 differentially expressed genes were identified in all the three datasets, including 72 up-regulated genes and 33 down-regulated genes in OCSCs compared with ovarian cancer cells. (Fig. 4A)

According to MCODE analysis, there were 3 clusters, including 3 nodes and 3 edges, 10 nodes and 13 edges and 9 nodes and 11edges respectively. MT1E and FBXO32 were seed genes of these clusters. The GSR, EEF1A1, IDH1, CLU, TGFB1, AKR1B1, MT1X and MT1E of top 10 key genes were included in these clusters. (Fig. 4B) Using STRING and cytoHubba, we had obtained the top 10 key genes of these DEGs, ranked by MCC degree. They were CAT, EGFR, GSR, EEF1A1, IDH1, CLU, TGFB1, AKR1B1, MT1X, MT1E. (Table 4, Fig. 4C)

Table 4

The top 10 key genes of the PPI network of the 105 DEGs, ranked by Maximal Clique Centrality (MCC) degree. The top 10 key genes were ranked by Maximal Clique Centrality (MCC) degree. The highest score was CAT. EEF1A1, IDH1, CLU, TGFB1 and AKR1B1 had equal scores and were ranked the forth. MT1X and MT1E had equal ratings and were all ranked the ninth.

Rank	Name	Fold change	Score
1	*CAT*	2.15	32
2	*EGFR*	-5.58	30
3	*GSR*	2.40	13
4	*EEF1A1*	2.13	8
4	*IDH1*	2.10	8
4	*CLU*	2.66	8
4	*TGFB1*	6.10	8
4	*AKR1B1*	26.08	8
9	*MT1X*	2.98	6
9	*MT1E*	3.44	6

KEGG pathway analysis indicated that these genes were significantly enriched in ‘FoxO signaling pathway’. 72 up-regulated genes were significantly enriched in ‘FoxO signaling pathway’, ‘Pentose and glucuronate interconversions’, ‘Mineral absorption’ and ‘Glutathione metabolism’. There were 2 KEGG pathways which the 33 down-expression genes were enriched in, such as ‘RNA transport’ and ‘Ras signaling pathway’, while the P value of the latter one is > 0.05. This might be due to the relatively small number of down-regulated genes. (Fig. 4D)

GO functional enrichment analysis on these genes indicated that these DEGs were significantly enriched in ‘negative regulation of cell proliferation’ (BP, GO:0008285), ‘cytosol’ (CC, GO:0005829) and ‘ferroxidase activity’ (MF, GO:0004322). 72 up-regulated genes were significantly enriched in ‘doxorubicin metabolic

process’ (BP, GO:0044597), ‘extracellular exosome’ (CC, GO:0070062) and ‘geranylgeranyl reductase activity’ (MF, GO:0045550). 33 down-regulated genes were significantly enriched in ‘intracellular ribonucleoprotein complex’ (CC, GO:0030529). Although they were enriched in ‘positive regulation of cell growth’ (BP, GO:0030307) and ‘poly(A) RNA binding’ (MF, GO:0044822), but the enrichments were not significant ($P > 0.05$). (Fig. 4E)

3.5 Construction of ceRNA regulatory network of OCSCs

21 DEGs were identified after combination of the 452 DEMs target genes and the 105 DEGs, including 11 up-regulated and 10 down-regulated DEGs. Finally, these DEGs were predicted as target genes for 10 of the 24 DEMs. Among them, the up-regulated miRNAs were miR-1287-5p, miR-193b-3p, miR-423-5p and miR-374b-5p, and the down-regulated miRNA were miR-425-5p, miR-96-5p, miR-26a-5p, miR-30e-5p, miR-183-5p and miR-146a-5p. A total of 25 transcripts of 13 lncRNA were predicted as the ceRNA of these miRNAs, including 21 up-regulated transcripts and 4 down-regulated ones. (Table 5, Supplementary Table 5) The obtained ceRNA regulatory network is shown in Fig. 5.

Table 5

MiRNAs, mRNAs and lncRNAs of the ceRNA network of OCSCs. The predicted ceRNA networks involved in stem cell characteristics maintenance of OCSCs are listed here. In fact, according to the differential expression results, miRNAs, lncRNAs and mRNAs listed here be constructed into ceRNAs. For example, the expression of miR-1287-5p was increased. According to the function of miRNA studied in the past, its target genes were more likely to be GFRA1 and EGFR with reduced expression, while its competitive endogenous RNA might be AC040162.3-201 rather than NEAT1-202.

miRNA	Predicted targets		lncRNA	
	up	down	up	down
miR-1287-5p up	*NRP2*	*GFRA1, EGFR*	*NEAT1-202*	*AC040162.3-201*
miR-193b-3p up	*TLE4, BCL6*	*CAMTA1, SLC7A5, LONRF1*	*NEAT1-202*	*LINC01184-208*
miR-423-5p up		*RASAL2*	*PVT1-212*	*SNHG20-203*
miR-374b-5p up	*AFF1*, *PAPD4*		*NEAT1-202*	
miR-425-5p down		*HNRNPD*	*MALAT1-201* *NEAT1-202*	
miR-96-5p down	*BRWD1, GNE, FBXO32*	*TNS3*, *GFRA1*	*MAPKAPK5-AS1-205* *MAPKAPK5-AS1-207* *MAPKAPK5-AS1-206* *MALAT1-201* *MAPKAPK5-AS1-204* *MAPKAPK5-AS1-201* *MALAT1-202*	

miRNA	Predicted targets		lncRNA	
	up	down	up	down
miR-26a-5p down	*ADM, PAPD4*	*ATP11C*	*LINC00665-207*	*LINC00665-205*
			GAS5-212	
			GAS5-206	
			LINC00665-202	
			MALAT1-202	
			LINC00665-204	
			NEAT1-202	
			SNHG5-210	
			SNHG5-206	
			SNHG5-202	
miR-30e-5p down	*PRDM1, PAPD4*	*RASAL2, HMGB3*	*LINC01089-210*	
			LINC01089-211	
			SNHG16-208	
			NEAT1-202	
			AC008124.1-201	
miR-183-5p down	*NRP2*		*NEAT1-202*	
miR-146a-5p down	*CASK, NRP2*	*HNRNPD*	*LINC00665-207*	
			NEAT1-202	

3.6 Preliminary validation of this bioinformatics research results

Through Kaplan-Meier (Km) curve analysis, there were 5 miRNAs, 12 mRNAs and 7 lncRNAs of which the differential expressions were significantly related to survival probability in ovarian cancer. (Supplementary Fig. 2) Among these genes, the most significantly related lncRNA was LINC00665, of which the expression was up regulated in OCSCs. According to the ceRNA network, one of LINC00665 transcripts was the ceRNA for miR-146a-5p, the expression of which had shown a downward trend in OCSCs in this study. QPCR had confirmed the microarray results. (Fig. 6A, for LINC00665, $p = 0.0002$, for miR-146a-5p, $p = 0.0001$) While the expression of NRP2 mRNA and protein, which was one of predicted target genes for miR-146a-5p, was higher than that in COC1. (Fig. 7C, D, $p = 0.0001$) LINC00665 was further overexpressed in COC1, and it was found that the proliferation ability of LINC00665 + COC1 was

increased, (Fig. 6B, $p = 0.0261$, $p = 0.0034$, $p = 0.0002$) and apoptosis was decreased. (Fig. 6D, $p < 0.0001$) However, compared with the NC group, the percentage of G0/G1 cells in LINC00665 overexpressed COC1 group showed a downward trend, but the difference was not statistically significant. (Fig. 6C, $p = 0.0278$) Km curve analysis showed that ovarian cancer patients with reduced miR-146a-5p expression had shorter survival time, while patients with reduced LINC00665 and NRP2 expression tended to have longer survival time. (Fig. 7A) The expression of miR-146a-5p was down-regulated after LINC00665 overexpressed in COC1, (Fig. 7B, $p = 0.0001$) and the expressions of NRP2 mRNA and protein were up-regulated in this kind of cells; (Fig. 7C, $p < 0.0001$) while the expression of LINC00665 was down-regulated in OCSCs, the expression of miR-146a-5p was up-regulated (Fig. 7B, $p = 0.0024$) and the expressions of NRP2 mRNA and protein were opposite to it. (Fig. 7C, $p < 0.0001$, D) According to TCGA data analysis, we observed significant upregulation of LINC00665 and significant downregulation of NRP2 in ovarian cancer. (Fig. 7A, for LINC00665, $p < 0.0001$, for NRP2, $p = 0.029$) In future studies, we need to further clarify the roles of LINC00665, miR-146a-5p and NRP2 in OCSCs and the regulatory relationships among them.

The procedure of our study was shown in Fig. 8.

4 Discussion

Failure of ovarian cancer treatment was often associated with the development of chemoresistance, including refractoriness (inherent resistance) and resistance (recurrence occurred within 6 months after response to complete treatment) (Na et al. 2009), which was more common in ovarian cancer chemotherapy. It is of great significance to study on the stem characteristic maintenance of OCSCs to clarify the formation and reversal of chemoresistance in ovarian cancer. The application of microarray technology and GEO database helps us to screen differential genes in OCSCs and to further find important genes related to maintain stem characteristics, to identify important regulatory genes that may influence drug resistance in ovarian cancer.

To construct important ceRNA regulatory networks, CD117+/CD133 + cells were first screened in the sphere from ovarian cancer cells COC1. The elevation of stem cell markers revealed that this group of cells had maintained stem cell conditions. The DEMs, DELs and DEGs between CD117+/CD133 + cells (OCSCs) and COC1 were further identified by microarray technology. Combining the microarray results with GEO datasets, we found that the target DEGs of DEMs of OCSCs were enriched in cancer related pathway, such as ‘Ras signaling pathway’, ‘p53 signaling pathway’, ‘AMPK signaling pathway’ and ‘FoxO signaling pathway’. It was suggested that these DEMs were involved in the regulation of the occurrence and development of OCSCs. While the DEGs of OCSCs were enriched in cancer related pathway, such as ‘FoxO signaling pathway’, ‘RNA transport’, ‘Pentose and glucuronate interconversions’, ‘Mineral absorption’ and ‘Glutathione metabolism’. It was also suggested that these DEGs were involved in the regulation of the occurrence and development of OCSCs by metabolic pathways. Combining with these two groups of DEGs had contributed to narrow the range of important mRNAs that regulate the characteristics of OCSCs. Meanwhile, lncRNAs that might be ceRNAs of these DEMs were found by bioinformatics analysis combined with lncRNA microarray result. Finally, 10 key (4 up-regulated and 6

down-regulated miRNAs) miRNAs and 21 predicted target mRNAs (11 up-regulated and 10 down-regulated mRNAs) were identified. 25 transcripts of 13 lncRNAs (21 up-regulated and 4 down-regulated transcripts) should be ceRNAs of these miRNAs. According to Km curve analysis, we found that the 5 DEMs, 12 DEGs and 7 DELs were significantly related to survival probability in ovarian cancer.

We selected the lncRNA with the highest correlation with survival probability, LINC00665, and its related miRNA, miR-146a-5p for preliminary study. QPCR confirmed microarray results that the expression of LINC00665 was increased and miR-146a-5p was decreased in OCSCs compared with COC1. Further regulation of the expression of LINC00665 indicated that LINC00665 was associated with cell proliferation and apoptosis in ovarian cancer cells. The target genes of miR-146a-5p in our ceRNA network included NRP2, CASK and HNRNPD, and the differential expression of these target genes was statistically significant with survival probability. However, the expression trend of HNRNPD was the same as that of miR-146a-5p, while among the three genes, the expression difference of NRP2 mRNA was the largest in our microarray result. And the expression of NRP2 mRNA and protein were increased in OCSCs compared with COC1 according to the results of qPCR and western blot. Therefore, we focused on analyzing the possible roles of miR-146a-5p, LINC00665 and NRP2 in the regulation of OCSCs stem cell characteristics in the following sections.

MiR-146a-5p is one of the anti-inflammatory miRNAs, which is considered to be a therapeutic target for inflammation-related diseases such as perinatal cardiomyopathy (Halkein et al. 2013) and obesity (Roos et al. 2016). It acts as a single miRNA regulatory factor inhibiting the function of regulatory T (Treg) cells, maintaining immune homeostasis of Treg cells, and its absence leads to IFNγ-dependent immune-mediated fatal lesions or tumors in a variety of organs (Lu et al. 2010; Mastroianni et al. 2019). Its rs2910164 SNP genotype may also influence the age of onset of cancer and is associated with early onset of cancer (Pastrello et al. 2010). The abnormal expression of miRNA-146a in CSCs has been found in many studies. And its effects in different tumors might be completely opposite (Shahriar et al. 2020). As an exosome miRNA in colorectal cancer, miR-146a-5p could target NUMB to activate wnt signaling pathway to generate and maintain cancer stem cells characteristics for promotion of tumor formation (Cheng et al. 2019b; Hwang and Yang 2016). While in cervical cancer and breast cancer CSCs, miR-146a-5p played a completely opposite role (Dong et al. 2019; Liang et al. 2018). It has been indicated that the expression of miR-146a-5p in tumors was also related to chemoresistance and metastasis of tumor cells (Shahriar et al. 2020). MiR-146a-5p could enhance the induction effect of platinum on apoptosis to prohibit cell proliferation in EOC cells (Cui et al. 2016; Li et al. 2017). Patients with lower expression of miR-146a-5p had reduced survival probability, shortened progression-free survival (PFS), and were prone to platinum chemoresistance (Wilczynski et al. 2017). A new study reported that lncRNA NR2F1-AS1 could act as a ceRNA by sponging miR-146a-5p/miR-877-5p to regulate the development of pancreatic ductal adenocarcinoma (PDAC). According to identify key target mRNAs by screening hub genes and coexpressed protein-coding genes (CEGs), it was found that NRP2 was not only one of the nine possible target genes that NR2F1-AS1 acted on, but also a possible target gene of miR-146a-5p. The researchers constructed a network in which NR2F1-AS1, as a ceRNA, competitively bound to miR-146a-5p/miR-877-5p to regulate the expression of nine target genes including NRP2 gene and participate in the regulation of

PDAC development(Luo et al. 2021). At present, there is no study on miR-146a-5p in OCSCs, but the miR-146a-5p derived from mesenchymal stem cells exosome has been reported to be able to enhance the sensitivity of ovarian cancer cells to docetaxel and taxane (Qiu et al. 2020). According to our study, miR-146a-5p might play an inhibitory role in OCSCs.

In another study, the researchers also predicted that there might be a ceRNA regulatory mechanism between miR-146a-5p and LINC00665, which was related to the prognosis of ovarian cancer (Gao et al. 2020). In our study, we have also found that a transcript of LINC00665 could be a ceRNA to participate in the regulation of miR-146a-5p on target genes. Studies on LINC00665 have been increasing in recent years. It has been considered to play an important regulatory role in various tumors. In 2018, Dong-Yue Wen et al. found an abnormally elevated LINC00665 expressed in hepatocellular carcinoma (HCC) data in the Cancer Genome Atlas (TCGA) database, which could interact with the cell cycle regulatory proteins to promote the development and progression of HCC(Wen et al. 2018). Following studies suggested that LINC00665, as the ceRNA of multiple miRNAs, could play an important role in the regulation of cell biological behaviors and chemoresistance in various malignant tumors (Cong et al. 2019; Liu et al. 2019; Qi et al. 2019; Shan and Li 2019; Yang et al. 2020). In high-grade serous ovarian cancer, a ceRNA regulatory network correlated with lymphocyte infiltration had been established by using TCGA, GTEx and GEO datasets, and it was suggested that LINC00665 was positively correlated with lymphocyte infiltration (Wu et al. 2020). LINC00665 also plays a role in tumor regulation by maintaining protein stability(Ding et al. 2020). Encoding small peptides is another way in which LINC00665 participates in the regulation of tumor progression (Guo et al. 2020). LINC00665 could also participate in the regulation of malignant biological behaviors of tumor cells by STAU1-mediated mRNA Degradation (SMD), which was an important post-transcriptional regulation of mRNA stability (Ruan et al. 2020). Our study found that the expression of LINC00665 was elevated in OCSCs. Ovarian cancer cells overexpressed with LINC00665 showed increased proliferation and decreased apoptosis, but the percentage of G0/G1 phase cells only showed a downward trend without statistical significance. Taking all the data together, we considered that LINC00665 might be involved in stemness maintenance of OCSCs as well as ovarian cancer cell proliferation. This requires us to further study the characteristic correlation between LINC00665 and OCSCs. In conclusion, LINC00665 has a clear regulatory role in many tumors, but there has been no study on its influence on the stem cell characteristics of CSCs, including OCSCs. In addition, we found that not all transcripts of LINC00665 showed an upward trend in the constructed ceRNA regulatory network. Therefore, the function of LINC00665 is worthy of further study.

NRP2 protein, a member of the NRPs family, is related to the development of the nervous system. It has the function of affecting signal receptors as a co-receptor. It is a transmembrane glycoprotein, which contains four extracellular domains capable of binding to ligands and one short cytoplasmic domain. Many microarray analyses revealed that NRP2 might be a hub gene for the development of a variety of tumors (Liu et al. 2018; Zhang et al. 2018; Zhu et al. 2018). Its function was either dependent or independent of the vascular endothelial growth factor receptor (VEGFR). Vascular endothelial growth factors (VEGFs) have the function of receptor tyrosine kinases activity to promote angiogenesis and increase vascular permeability by binding with VEGFR and are involved in maintaining the stem cell

characteristics of CSCs in many tumors (Krishnapriya et al. 2019; Lim et al. 2014). While the co-receptor NRP2 can form a complex with VEGFR to enhance its affinity with VEGF and enhance tumor-promoting effect of VEGF (Neufeld et al. 2002). In addition, NRP2 can bind to integrins to regulate CSCs generation and stem characteristics maintenance through VEGF/NRP2 signaling (Goel et al. 2014; Goel et al. 2013; Goel et al. 2012). At present, most of anti-VEGF drugs (such as bevacizumab), which only block the binding of VEGF and VEGFR but not NRP2, cannot inhibit CSCs effectively, but promote the enrichment (Geretti et al. 2010). Therefore, in addition to anti-VEGF therapy, combining anti-VEGF/NRP2 therapy may enhance the benefits of anti-VEGF therapy alone (Goel et al. 2016). NRP2 can also act without VEGF signaling in CSCs. It has been indicated that NRP2 could bind to PDZ protein through PDZ domain in its cytoplasmic part, participating in receptor transport and signal transduction in tumor development regulation (Katoh 2013). Other studies have shown that NRP2b, an alternative splicing isomer of NRP2, could bind to PTEN to increase the resistance of non-small-cell lung cancer (NSCLC) cells to EGFR inhibitor gefitinib (Gemmill et al. 2017). Although NRP2 wasn't the hub genes of PPI networks according to our analysis, but the up-regulated trend was the most obvious among mRNA in the ceRNA network in OCSCs. Km curve suggested that the survival probability of patients with high NRP2 expression decreased faster than that of patients with low expression. All the above suggested the importance of NRP2 in tumor development. According to our study, although analysis of TCGA and GTEx data showed that NRP2 expression was downregulated in ovarian cancer, its expression was elevated in microarray analysis comparing differential genes in ovarian cancer cells and OCSCs. And our experiment also confirmed this. It's suggested that NRP2 might play an important role in maintaining the stem cell characteristics of OCSCs. We further regulated the expression of LINC00665 and found that NRP2 mRNA and protein expression were positively correlated with LINC00665 expression. Further study of the ceRNA mechanism regulating NRP2 expression in OCSCs can better reveal the mechanism of stem cell characteristics maintenance in OCSCs.

5 Conclusion

CeRNA is an important post-transcriptional regulation mode of genes. At present, studies on ceRNA regulation in various CSCs have been carried out extensively. However, as one of cancer stem cell-related tumors, the establishment of ceRNA regulatory network in ovarian cancer hasn't been established yet. According to our study, a ceRNA regulatory network of OCSCs has been initially established by microarray analysis and bioinformatics research, but further clinical and molecular biology studies are required. In the ceRNA network constructed, it was indicated that the protein encoding genes had less direct interaction with each other according to PPI constructed by STRING and Cytoscape. However, through the construction of ceRNA network, these protein encoding genes with no direct interactions were connected indirectly by lncRNA-miRNA-mRNA network. Our further studies are expected to find out the important sites and regulatory ways to maintain the characteristics of stem cells in OCSCs, providing new theoretical basis and experimental guarantee for ovarian cancer research.

Declarations

Acknowledgments

This study was supported by grants from the National Natural Science Foundation of China for Young Scientists of China (Grant No. 81902658).

Conflict of interest

Authors declare no conflict of interest.

Author contributions

Yingying Zhou: Conceptualization, Methodology, Software, Supervision, Funding acquisition. Zhen Li: Data curation, Writing-Original draft preparation. Zhijiao Wang: Resources, Writing- Reviewing and Editing.

References

1. Agarwal V, Bell GW, Nam JW, Bartel DP (2015) Predicting effective microRNA target sites in mammalian mRNAs. Elife 4. https://doi.org/10.7554/eLife.05005
2. Aletti GD, Gallenberg MM, Cliby WA, Jatoi A, Hartmann LC (2007) Current management strategies for ovarian cancer. Mayo Clin Proc 82:751–770. https://doi.org/10.4065/82.6.751
3. Alvero AB, Chen R, Fu HH, Montagna M, Schwartz PE, Rutherford T, Silasi DA, Steffensen KD, Waldstrom M, Visintin I et al. (2009) Molecular phenotyping of human ovarian cancer stem cells unravels the mechanisms for repair and chemoresistance. Cell Cycle 8:158–166. https://doi.org/10.4161/cc.8.1.7533
4. Braga EA, Fridman MV, Moscovtsev AA, Filippova EA, Dmitriev AA, Kushlinskii NE (2020) LncRNAs in Ovarian Cancer Progression, Metastasis, and Main Pathways: ceRNA and Alternative Mechanisms. Int J Mol Sci 21. https://doi.org/10.3390/ijms21228855
5. Chen K, Rajewsky N (2006) Natural selection on human microRNA binding sites inferred from SNP data. Nat Genet 38:1452–1456. https://doi.org/10.1038/ng1910
6. Cheng FHC, Lin HY, Hwang TW, Chen YC, Huang RL, Chang CB, Yang W, Lin RI, Lin CW, Chen GCW et al. (2019a) E2F6 functions as a competing endogenous RNA, and transcriptional repressor, to promote ovarian cancer stemness. Cancer Sci 110:1085–1095. https://doi.org/10.1111/cas.13920
7. Cheng WC, Liao TT, Lin CC, Yuan LE, Lan HY, Lin HH, Teng HW, Chang HC, Lin CH, Yang CY et al. (2019b) RAB27B-activated secretion of stem-like tumor exosomes delivers the biomarker microRNA-146a-5p, which promotes tumorigenesis and associates with an immunosuppressive tumor microenvironment in colorectal cancer. Int J Cancer 145:2209–2224. https://doi.org/10.1002/ijc.32338
8. Clarke MF, Dick JE, Dirks PB, Eaves CJ, Jamieson CH, Jones DL, Visvader J, Weissman IL, Wahl GM (2006) Cancer stem cells–perspectives on current status and future directions: AACR Workshop on cancer stem cells. Cancer Res 66:9339–9344. https://doi.org/10.1158/0008-5472.can-06-3126

9. Cong Z, Diao Y, Xu Y, Li X, Jiang Z, Shao C, Ji S, Shen Y, De W, Qiang Y (2019) Long non-coding RNA linc00665 promotes lung adenocarcinoma progression and functions as ceRNA to regulate AKR1B10-ERK signaling by sponging miR-98. Cell Death Dis 10:84. https://doi.org/10.1038/s41419-019-1361-3
10. Cui Y, She K, Tian D, Zhang P, Xin X (2016) miR-146a Inhibits Proliferation and Enhances Chemosensitivity in Epithelial Ovarian Cancer via Reduction of SOD2. Oncol Res 23:275–282. https://doi.org/10.3727/096504016x14562725373798
11. Dalerba P, Cho RW, Clarke MF (2007) Cancer stem cells: models and concepts. Annu Rev Med 58:267–284. https://doi.org/10.1146/annurev.med.58.062105.204854
12. Ding J, Zhao J, Huan L, Liu Y, Qiao Y, Wang Z, Chen Z, Huang S, Zhao Y, He X (2020) Inflammation-induced LINC00665 increases the malignancy through activating PKR/NF-kappaB pathway in hepatocellular carcinoma. Hepatology. https://doi.org/10.1002/hep.31195
13. Dong Z, Yu C, Rezhiya K, Gulijiahan A, Wang X (2019) Downregulation of miR-146a promotes tumorigenesis of cervical cancer stem cells via VEGF/CDC42/PAK1 signaling pathway. Artif Cells Nanomed Biotechnol 47:3711–3719. https://doi.org/10.1080/21691401.2019.1664560
14. Gao L, Li X, Nie X, Guo Q, Liu Q, Qi Y, Liu J, Lin B (2020) Construction of novel mRNA-miRNA-lncRNA regulatory networks associated with prognosis of ovarian cancer. 107150/jca49557 11:7057–7072. https://doi.org/10.7150/jca.49557
15. Gemmill RM, Nasarre P, Nair-Menon J, Cappuzzo F, Landi L, D'Incecco A, Uramoto H, Yoshida T, Haura EB, Armeson K et al. (2017) The neuropilin 2 isoform NRP2b uniquely supports TGFbeta-mediated progression in lung cancer. Sci Signal 10. https://doi.org/10.1126/scisignal.aag0528
16. Geretti E, van Meeteren LA, Shimizu A, Dudley AC, Claesson-Welsh L, Klagsbrun M (2010) A mutated soluble neuropilin-2 B domain antagonizes vascular endothelial growth factor bioactivity and inhibits tumor progression. Mol Cancer Res 8:1063–1073. https://doi.org/10.1158/1541-7786.mcr-10-0157
17. Goel HL, Gritsko T, Pursell B, Chang C, Shultz LD, Greiner DL, Norum JH, Toftgard R, Shaw LM, Mercurio AM (2014) Regulated splicing of the alpha6 integrin cytoplasmic domain determines the fate of breast cancer stem cells. Cell Rep 7:747–761. https://doi.org/10.1016/j.celrep.2014.03.059
18. Goel HL, Pursell B, Chang C, Shaw LM, Mao J, Simin K, Kumar P, Vander Kooi CW, Shultz LD, Greiner DL et al. (2013) GLI1 regulates a novel neuropilin-2/alpha6beta1 integrin based autocrine pathway that contributes to breast cancer initiation. EMBO Mol Med 5:488–508. https://doi.org/10.1002/emmm.201202078
19. Goel HL, Pursell B, Shultz LD, Greiner DL, Brekken RA, Vander Kooi CW, Mercurio AM (2016) P-Rex1 Promotes Resistance to VEGF/VEGFR-Targeted Therapy in Prostate Cancer. Cell Rep 14:2193–2208. https://doi.org/10.1016/j.celrep.2016.02.016
20. Goel HL, Pursell B, Standley C, Fogarty K, Mercurio AM (2012) Neuropilin-2 regulates alpha6beta1 integrin in the formation of focal adhesions and signaling. J Cell Sci 125:497–506. https://doi.org/10.1242/jcs.094433

21. Guo B, Wu S, Zhu X, Zhang L, Deng J, Li F, Wang Y, Zhang S, Wu R, Lu J et al. (2020) Micropeptide CIP2A-BP encoded by LINC00665 inhibits triple-negative breast cancer progression. EMBO J 39:e102190. https://doi.org/10.15252/embj.2019102190
22. Halkein J, Tabruyn SP, Ricke-Hoch M, Haghikia A, Nguyen NQ, Scherr M, Castermans K, Malvaux L, Lambert V, Thiry M et al. (2013) MicroRNA-146a is a therapeutic target and biomarker for peripartum cardiomyopathy. J Clin Invest 123:2143–2154. https://doi.org/10.1172/jci64365
23. Han Q, Wu W, Cui Y (2020) LINC00337 Regulates KLF5 and Maintains Stem-Cell Like Traits of Cervical Cancer Cells by Modulating miR-145. Front Oncol 10:1433. https://doi.org/10.3389/fonc.2020.01433
24. Huang da W, Sherman BT, Lempicki RA (2009a) Bioinformatics enrichment tools: paths toward the comprehensive functional analysis of large gene lists. Nucleic Acids Res 37:1–13. https://doi.org/10.1093/nar/gkn923
25. Huang da W, Sherman BT, Lempicki RA (2009b) Systematic and integrative analysis of large gene lists using DAVID bioinformatics resources. Nat Protoc 4:44–57. https://doi.org/10.1038/nprot.2008.211
26. Hwang WL, Yang MH (2016) Numb is involved in the non-random segregation of subcellular vesicles in colorectal cancer stem cells. Cell Cycle 15:2697–2703. https://doi.org/10.1080/15384101.2016.1218101
27. Katoh M (2013) Functional proteomics, human genetics and cancer biology of GIPC family members. Exp Mol Med 45:e26. https://doi.org/10.1038/emm.2013.49
28. Krishnapriya S, Sidhanth C, Manasa P, Sneha S, Bindhya S, Nagare RP, Ramachandran B, Vishwanathan P, Murhekar K, Shirley S et al. (2019) Cancer stem cells contribute to angiogenesis and lymphangiogenesis in serous adenocarcinoma of the ovary. Angiogenesis 22:441–455. https://doi.org/10.1007/s10456-019-09669-x
29. Kwon MJ, Shin YK (2011) Epigenetic regulation of cancer-associated genes in ovarian cancer. Int J Mol Sci 12:983–1008. https://doi.org/10.3390/ijms12020983
30. Lee HH, Bellat V, Law B (2017) Chemotherapy induces adaptive drug resistance and metastatic potentials via phenotypic CXCR4-expressing cell state transition in ovarian cancer. PLoS One 12:e0171044. https://doi.org/10.1371/journal.pone.0171044
31. Lee YJ, Wu CC, Li JW, Ou CC, Hsu SC, Tseng HH, Kao MC, Liu JY (2016) A rational approach for cancer stem-like cell isolation and characterization using CD44 and prominin-1(CD133) as selection markers. Oncotarget 7:78499–78515. https://doi.org/10.18632/oncotarget.12100
32. Li JH, Liu S, Zhou H, Qu LH, Yang JH (2014) starBase v2.0: decoding miRNA-ceRNA, miRNA-ncRNA and protein-RNA interaction networks from large-scale CLIP-Seq data. Nucleic Acids Res 42:D92-97. https://doi.org/10.1093/nar/gkt1248
33. Li X, Jin Y, Mu Z, Chen W, Jiang S (2017) MicroRNA146a5p enhances cisplatininduced apoptosis in ovarian cancer cells by targeting multiple antiapoptotic genes. Int J Oncol 51:327–335. https://doi.org/10.3892/ijo.2017.4023

34. Liang R, Li Y, Wang M, Tang SC, Xiao G, Sun X, Li G, Du N, Liu D, Ren H (2018) MiR-146a promotes the asymmetric division and inhibits the self-renewal ability of breast cancer stem-like cells via indirect upregulation of Let-7. Cell Cycle 17:1445–1456. https://doi.org/10.1080/15384101.2018.1489176
35. Lim JJ, Yang K, Taylor-Harding B, Wiedemeyer WR, Buckanovich RJ (2014) VEGFR3 inhibition chemosensitizes ovarian cancer stemlike cells through down-regulation of BRCA1 and BRCA2. Neoplasia 16:343–353 e341-342. https://doi.org/10.1016/j.neo.2014.04.003
36. Liu B, Yang H, Taher L, Denz A, Grutzmann R, Pilarsky C, Weber GF (2018) Identification of Prognostic Biomarkers by Combined mRNA and miRNA Expression Microarray Analysis in Pancreatic Cancer. Transl Oncol 11:700–714. https://doi.org/10.1016/j.tranon.2018.03.003
37. Liu X, Lu X, Zhen F, Jin S, Yu T, Zhu Q, Wang W, Xu K, Yao J, Guo R (2019) LINC00665 Induces Acquired Resistance to Gefitinib through Recruiting EZH2 and Activating PI3K/AKT Pathway in NSCLC. Mol Ther Nucleic Acids 16:155–161. https://doi.org/10.1016/j.omtn.2019.02.010
38. Lu LF, Boldin MP, Chaudhry A, Lin LL, Taganov KD, Hanada T, Yoshimura A, Baltimore D, Rudensky AY (2010) Function of miR-146a in controlling Treg cell-mediated regulation of Th1 responses. Cell 142:914–929. https://doi.org/10.1016/j.cell.2010.08.012
39. Luo D, Liu Y, Li Z, Zhu H, Yu X (2021) NR2F1-AS1 Promotes Pancreatic Ductal Adenocarcinoma Progression Through Competing Endogenous RNA Regulatory Network Constructed by Sponging miRNA-146a-5p/miRNA-877-5p. 103389/fcell2021736980 9:736980. https://doi.org/10.3389/fcell.2021.736980
40. Luo L, Zeng J, Liang B, Zhao Z, Sun L, Cao D, Yang J, Shen K (2011) Ovarian cancer cells with the CD117 phenotype are highly tumorigenic and are related to chemotherapy outcome. Exp Mol Pathol 91:596–602. https://doi.org/10.1016/j.yexmp.2011.06.005
41. Ma L, Lai D, Liu T, Cheng W, Guo L (2010) Cancer stem-like cells can be isolated with drug selection in human ovarian cancer cell line SKOV3. Acta Biochim Biophys Sin (Shanghai) 42:593–602. https://doi.org/10.1093/abbs/gmq067
42. Mastroianni J, Stickel N, Andrlova H, Hanke K, Melchinger W, Duquesne S, Schmidt D, Falk M, Andrieux G, Pfeifer D et al. (2019) miR-146a Controls Immune Response in the Melanoma Microenvironment. Cancer Res 79:183–195. https://doi.org/10.1158/0008-5472.can-18-1397
43. Moore N, Lyle S (2011) Quiescent, slow-cycling stem cell populations in cancer: a review of the evidence and discussion of significance. J Oncol 2011. https://doi.org/10.1155/2011/396076
44. Morrison SJ, Kimble J (2006) Asymmetric and symmetric stem-cell divisions in development and cancer. Nature 441:1068–1074. https://doi.org/10.1038/nature04956
45. Na YJ, Farley J, Zeh A, del Carmen M, Penson R, Birrer MJ (2009) Ovarian cancer: markers of response. Int J Gynecol Cancer 19 Suppl 2:S21-29. https://doi.org/10.1111/igc.0b013e3181c2aeb5
46. Nagy A, Lanczky A, Menyhart O, Gyorffy B (2018) Validation of miRNA prognostic power in hepatocellular carcinoma using expression data of independent datasets. Sci Rep 8:9227. https://doi.org/10.1038/s41598-018-27521-y

47. Neufeld G, Kessler O, Herzog Y (2002) The interaction of Neuropilin-1 and Neuropilin-2 with tyrosine-kinase receptors for VEGF. Adv Exp Med Biol 515:81–90. https://doi.org/10.1007/978-1-4615-0119-0_7
48. Paraskevopoulou MD, Georgakilas G, Kostoulas N, Reczko M, Maragkakis M, Dalamagas TM, Hatzigeorgiou AG (2013) DIANA-LncBase: experimentally verified and computationally predicted microRNA targets on long non-coding RNAs. Nucleic Acids Res 41:D239-245. https://doi.org/10.1093/nar/gks1246
49. Pastrello C, Polesel J, Della Puppa L, Viel A, Maestro R (2010) Association between hsa-mir-146a genotype and tumor age-of-onset in BRCA1/BRCA2-negative familial breast and ovarian cancer patients. Carcinogenesis 31:2124–2126. https://doi.org/10.1093/carcin/bgq184
50. Qi H, Xiao Z, Wang Y (2019) Long non-coding RNA LINC00665 gastric cancer tumorigenesis by regulation miR-149-3p/RNF2 axis. Onco Targets Ther 12:6981–6990. https://doi.org/10.2147/ott.s214588
51. Qiu L, Wang J, Chen M, Chen F, Tu W (2020) Exosomal microRNA146a derived from mesenchymal stem cells increases the sensitivity of ovarian cancer cells to docetaxel and taxane via a LAMC2mediated PI3K/Akt axis. Int J Mol Med 46:609–620. https://doi.org/10.3892/ijmm.2020.4634
52. Roos J, Enlund E, Funcke JB, Tews D, Holzmann K, Debatin KM, Wabitsch M, Fischer-Posovszky P (2016) miR-146a-mediated suppression of the inflammatory response in human adipocytes. Sci Rep 6:38339. https://doi.org/10.1038/srep38339
53. Ruan X, Zheng J, Liu X, Liu Y, Liu L, Ma J, He Q, Yang C, Wang D, Cai H et al. (2020) lncRNA LINC00665 Stabilized by TAF15 Impeded the Malignant Biological Behaviors of Glioma Cells via STAU1-Mediated mRNA Degradation. Mol Ther Nucleic Acids 20:823–840. https://doi.org/10.1016/j.omtn.2020.05.003
54. Sanchez-Garcia I, Vicente-Duenas C, Cobaleda C (2007) The theoretical basis of cancer-stem-cell-based therapeutics of cancer: can it be put into practice? Bioessays 29:1269–1280. https://doi.org/10.1002/bies.20679
55. Schmohl JU, Vallera DA (2016) CD133, Selectively Targeting the Root of Cancer. Toxins (Basel) 8. https://doi.org/10.3390/toxins8060165
56. Sethupathy P, Corda B, Hatzigeorgiou AG (2006) TarBase: A comprehensive database of experimentally supported animal microRNA targets. RNA 12:192–197. https://doi.org/10.1261/rna.2239606
57. Shahriar A, Ghaleh-Aziz Shiva G, Ghader B, Farhad J, Hosein A, Parsa H (2020) The dual role of mir-146a in metastasis and disease progression. Biomed Pharmacother 126:110099. https://doi.org/10.1016/j.biopha.2020.110099
58. Shan Y, Li P (2019) Long Intergenic Non-Protein Coding RNA 665 Regulates Viability, Apoptosis, and Autophagy via the MiR-186-5p/MAP4K3 Axis in Hepatocellular Carcinoma. Yonsei Med J 60:842–853. https://doi.org/10.3349/ymj.2019.60.9.842

59. Shannon P, Markiel A, Ozier O, Baliga NS, Wang JT, Ramage D, Amin N, Schwikowski B, Ideker T (2003) Cytoscape: a software environment for integrated models of biomolecular interaction networks. Genome Res 13:2498–2504. https://doi.org/10.1101/gr.1239303
60. Siegel RL, Miller KD, Jemal A (2016) Cancer statistics, 2016. CA Cancer J Clin 66:7–30. https://doi.org/10.3322/caac.21332
61. Siegel RL, Miller KD, Jemal A (2019) Cancer statistics, 2019. CA Cancer J Clin 69:7–34. https://doi.org/10.3322/caac.21551
62. Snel B, Lehmann G, Bork P, Huynen MA (2000) STRING: a web-server to retrieve and display the repeatedly occurring neighbourhood of a gene. Nucleic Acids Res 28:3442–3444. https://doi.org/10.1093/nar/28.18.3442
63. Szotek PP, Pieretti-Vanmarcke R, Masiakos PT, Dinulescu DM, Connolly D, Foster R, Dombkowski D, Preffer F, Maclaughlin DT, Donahoe PK (2006) Ovarian cancer side population defines cells with stem cell-like characteristics and Mullerian Inhibiting Substance responsiveness. Proc Natl Acad Sci U S A 103:11154–11159. https://doi.org/10.1073/pnas.0603672103
64. Teramura T, Fukuda K, Kurashimo S, Hosoi Y, Miki Y, Asada S, Hamanishi C (2008) Isolation and characterization of side population stem cells in articular synovial tissue. BMC Musculoskelet Disord 9:86. https://doi.org/10.1186/1471-2474-9-86
65. Valent P, Bonnet D, De Maria R, Lapidot T, Copland M, Melo JV, Chomienne C, Ishikawa F, Schuringa JJ, Stassi G et al. (2012) Cancer stem cell definitions and terminology: the devil is in the details. Nat Rev Cancer 12:767–775. https://doi.org/10.1038/nrc3368
66. Wen DY, Lin P, Pang YY, Chen G, He Y, Dang YW, Yang H (2018) Expression of the Long Intergenic Non-Protein Coding RNA 665 (LINC00665) Gene and the Cell Cycle in Hepatocellular Carcinoma Using The Cancer Genome Atlas, the Gene Expression Omnibus, and Quantitative Real-Time Polymerase Chain Reaction. Med Sci Monit 24:2786–2808. https://doi.org/10.12659/msm.907389
67. Wilczynski M, Zytko E, Szymanska B, Dzieniecka M, Nowak M, Danielska J, Stachowiak G, Wilczynski JR (2017) Expression of miR-146a in patients with ovarian cancer and its clinical significance. Oncol Lett 14:3207–3214. https://doi.org/10.3892/ol.2017.6477
68. Wu M, Shang X, Sun Y, Wu J, Liu G (2020) Integrated analysis of lymphocyte infiltration-associated lncRNA for ovarian cancer via TCGA, GTEx and GEO datasets. PeerJ 8:e8961. https://doi.org/10.7717/peerj.8961
69. Yan HC, Fang LS, Xu J, Qiu YY, Lin XM, Huang HX, Han QY (2014) The identification of the biological characteristics of human ovarian cancer stem cells. Eur Rev Med Pharmacol Sci 18:3497–3503
70. Yang B, Bai Q, Chen H, Su K, Gao C (2020) LINC00665 induces gastric cancer progression through activating Wnt signaling pathway. J Cell Biochem 121:2268–2276. https://doi.org/10.1002/jcb.29449
71. Yang B, Yan X, Liu L, Jiang C, Hou S (2017) Overexpression of the cancer stem cell marker CD117 predicts poor prognosis in epithelial ovarian cancer patients: evidence from meta-analysis. Onco Targets Ther 10:2951–2961. https://doi.org/10.2147/ott.s136549

72. Zhang S, Balch C, Chan MW, Lai HC, Matei D, Schilder JM, Yan PS, Huang TH, Nephew KP (2008) Identification and characterization of ovarian cancer-initiating cells from primary human tumors. Cancer Res 68:4311–4320. https://doi.org/10.1158/0008-5472.can-08-0364
73. Zhang Y, Zhang R, Ding X, Ai K (2018) EFNB2 acts as the target of miR-557 to facilitate cell proliferation, migration and invasion in pancreatic ductal adenocarcinoma by bioinformatics analysis and verification. Am J Transl Res 10:3514–3528
74. Zhu L, Shu Z, Sun X (2018) Bioinformatic analysis of four miRNAs relevant to metastasis-regulated processes in endometrial carcinoma. Cancer Manag Res 10:2337–2346. https://doi.org/10.2147/cmar.s168594

Figures

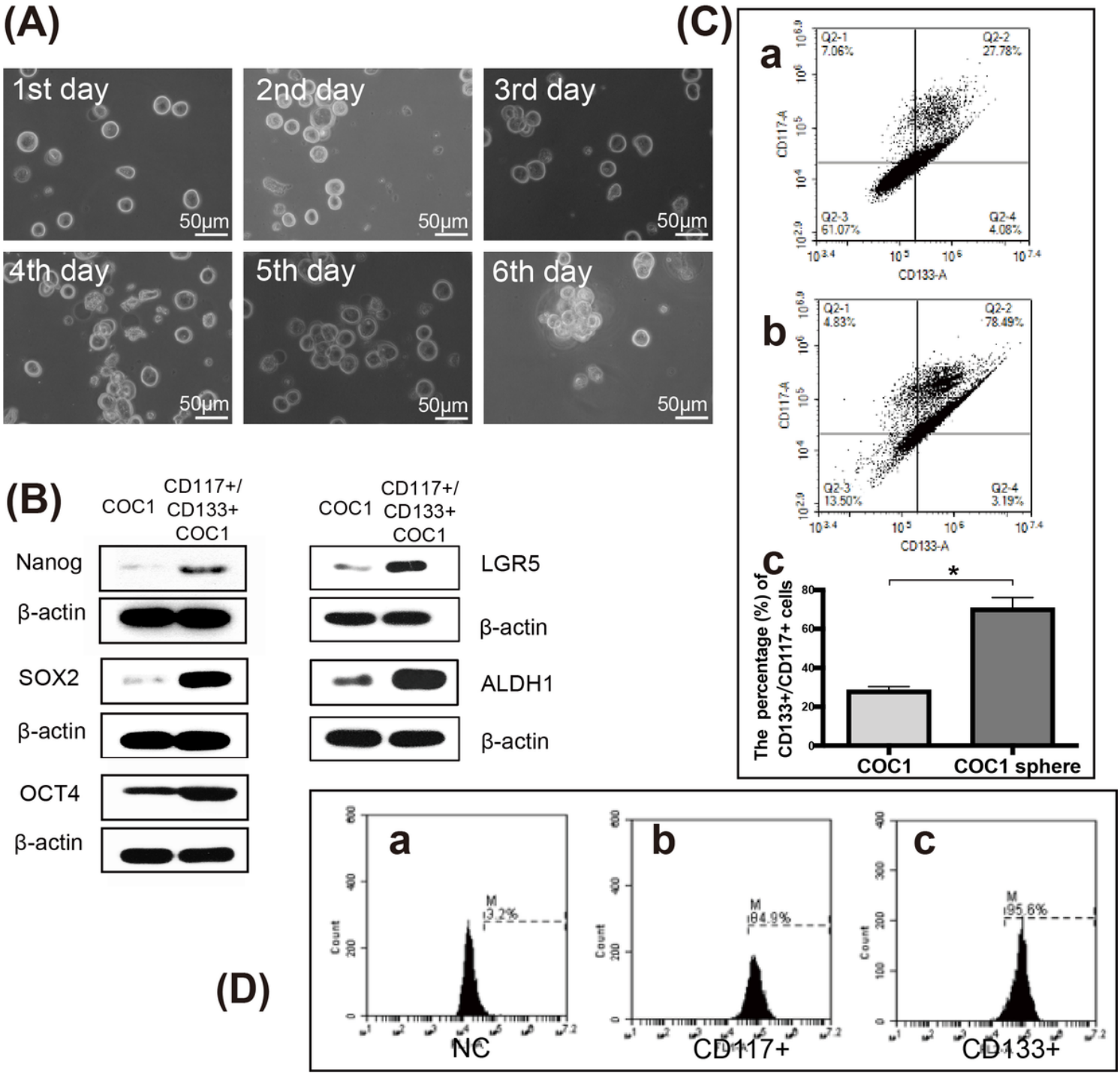

Figure 1

The sorting of ovarian cancer stem cell-like cells (OCSCs) and the detection results of stem cell markers.

(A) sphere formation in COC1 after treatment by stem cell conditions, (B) detection of differences in expression of stem cell markers in COC1 after treatment by Western blot. Detection of the percentage of CD117+/CD133+ cells in COC1 after treatment by flow cytometry: (C) a, COC1, b, CD117+/CD133+ cells, c, the comparison of the percentage of CD133+/CD117+ expression cells in COC1 and COC1 sphere; (D) a, COC1, b, CD117+ cells, c, CD133+ cells.

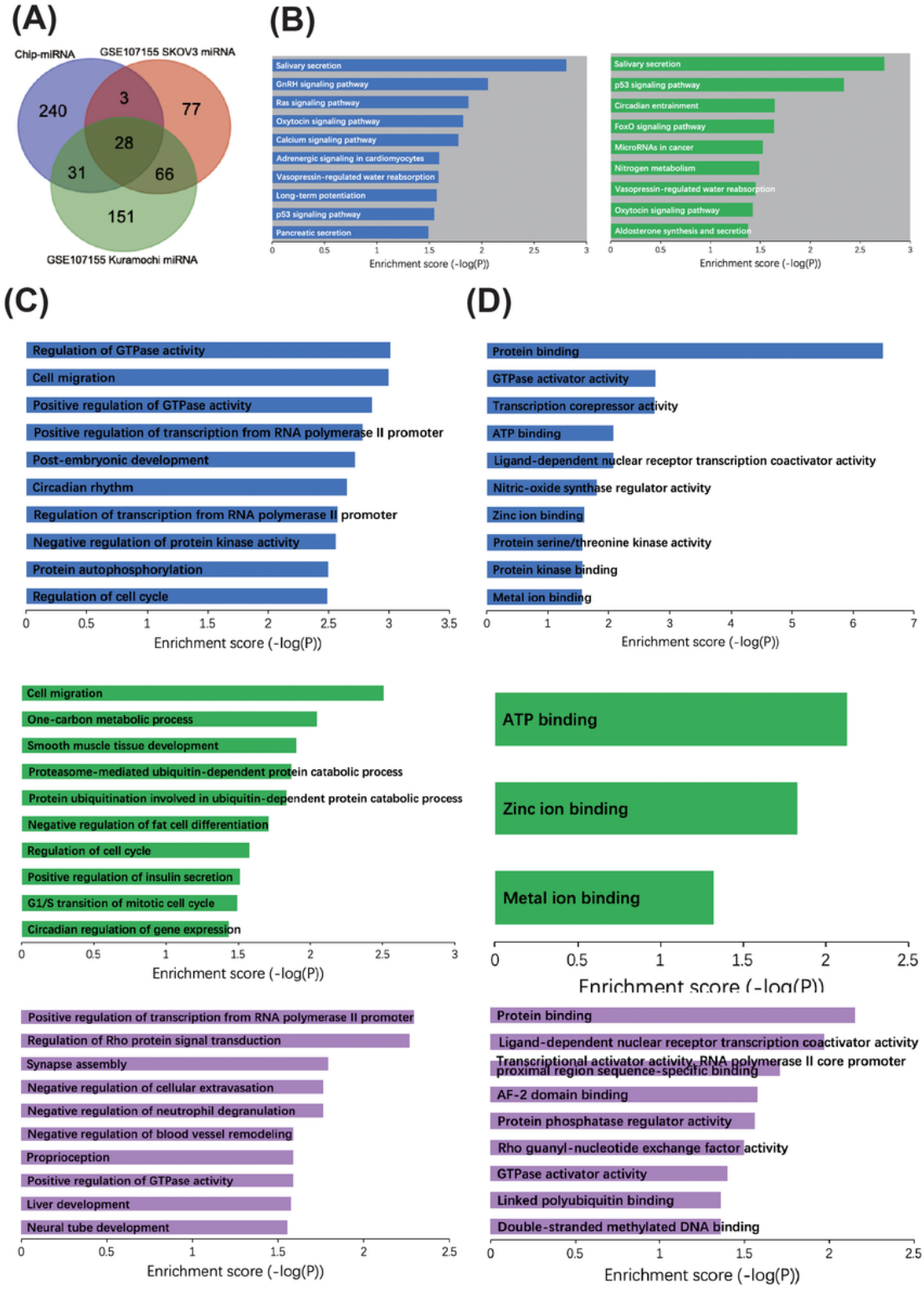

Figure 2

Identification of DEMs in miRNA microarray, GSE107155-SKOV3 and GSE107155-Kuramochi datasets. The enrichment analysis of corresponding target DEGs in GO and KEGG pathways.

(A) Combined with the results of microarray and GEO datasets, 28 DEMs were identified that were differentially expressed in all datasets, (B) KEGG pathway enrichment analysis of corresponding target

DEGs, (C) biological process enrichment analysis of corresponding target DEGs, (D) molecular function enrichment analysis of corresponding target DEGs. The blue bars represented all DEGs, the green ones represented up-regulated DEGs, and the purple ones represented down-regulated DEGs.

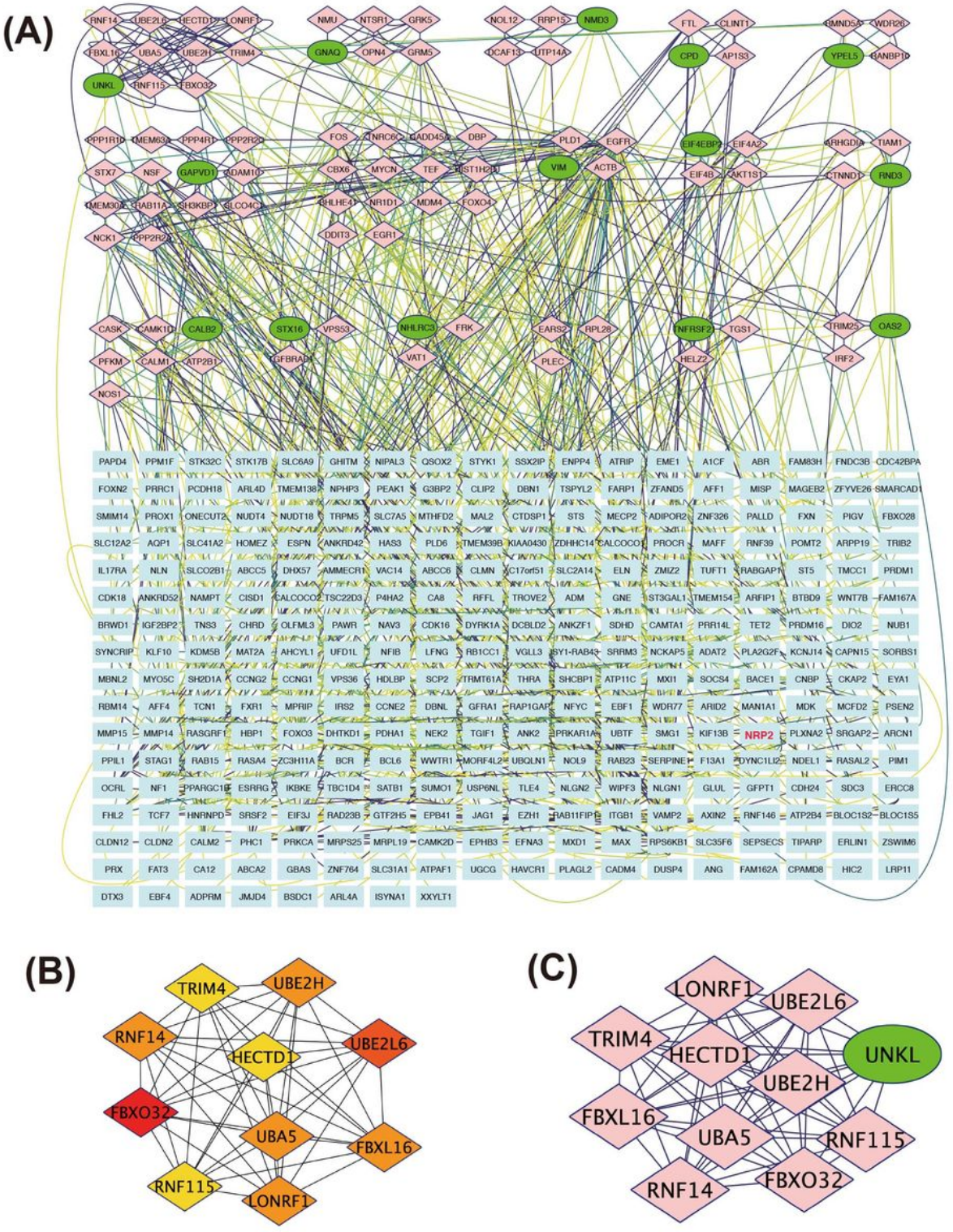

Figure 3

Constructed PPI network by STRING and cytoHubba.

(A) PPI network was constructed for 452 predicted target DEGs of the 24 DEMs mentioned above by STRING, (B) the top 10 key genes ranked by MCC degree, (C) the most significant cluster including 11 nodes and 55 edges according to MCODE analysis.

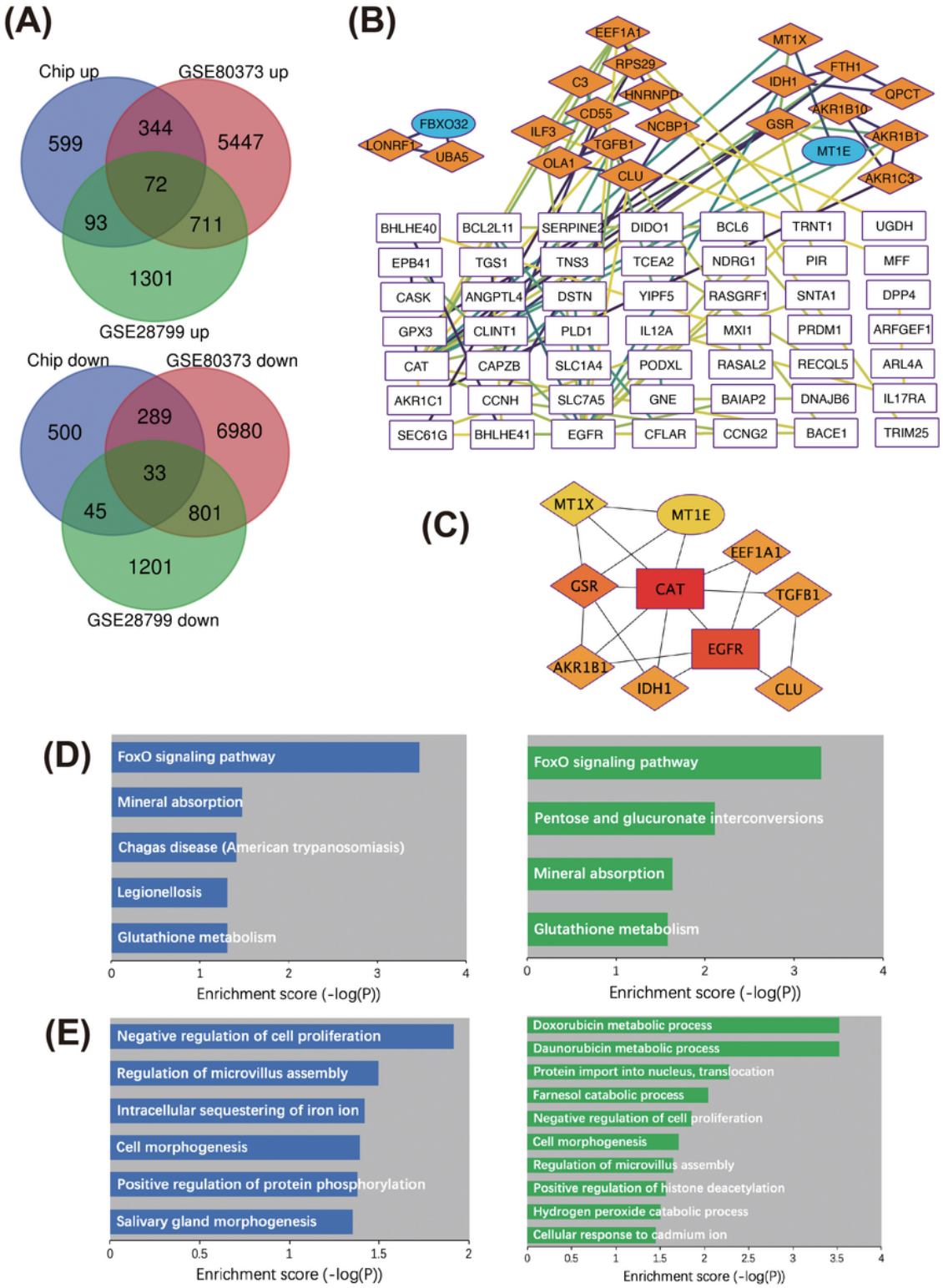

Figure 4

Identification of DEGs in miRNA microarray, GSE80373 and GSE28799 datasets, and the results of PPI, KEGG and GO analysis for these DEGs.

(A) The venn diagram on the top was for up-regulated genes, while the bottom one was for down-regulated gene, (B) constructed PPI network by STRING and cytoHubba, DEGs not participating in PPI network were not shown, (C) the top 10 key genes of the PPI network ranked by MCC degree, (D) KEGG pathway and (E) biological process enrichment analysis of this group of DEGs. The blue bars represented all 105 DEGs, and the green ones represented 77 up-regulated ones of the 105 DEGs.

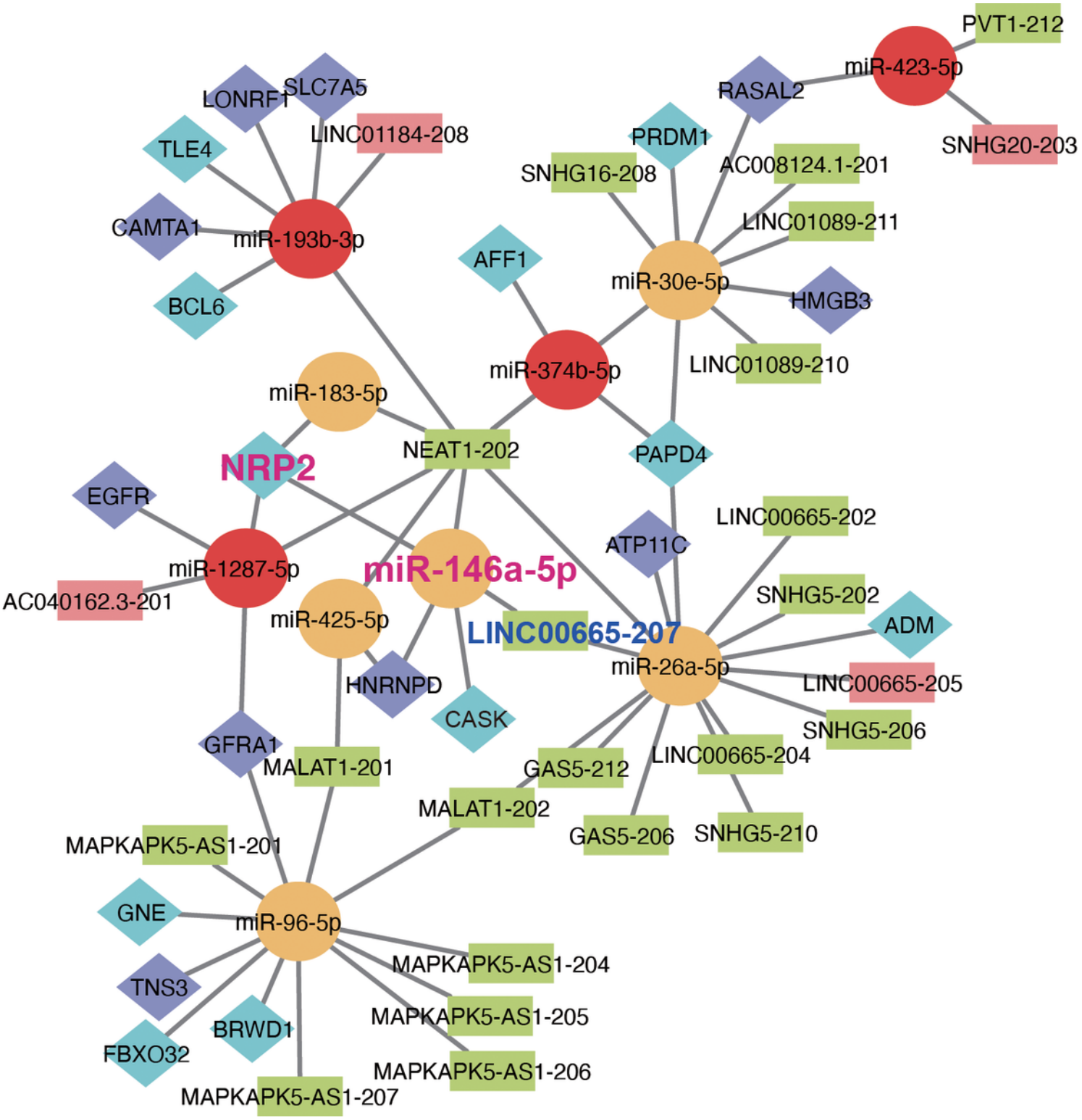

Figure 5

The final ceRNA regulatory network in OCSCs.

The circles represent DEMs, red represents DEMs with increased expression, and yellow represents DEMs with decreased expression. The rectangles represent DELs, green represents DELs with increased

expression and pink represents DELs with decreased expression. The diamonds represent DEGs, blue represents DEGs with increased expression and purple represents DEGs with decreased expression.

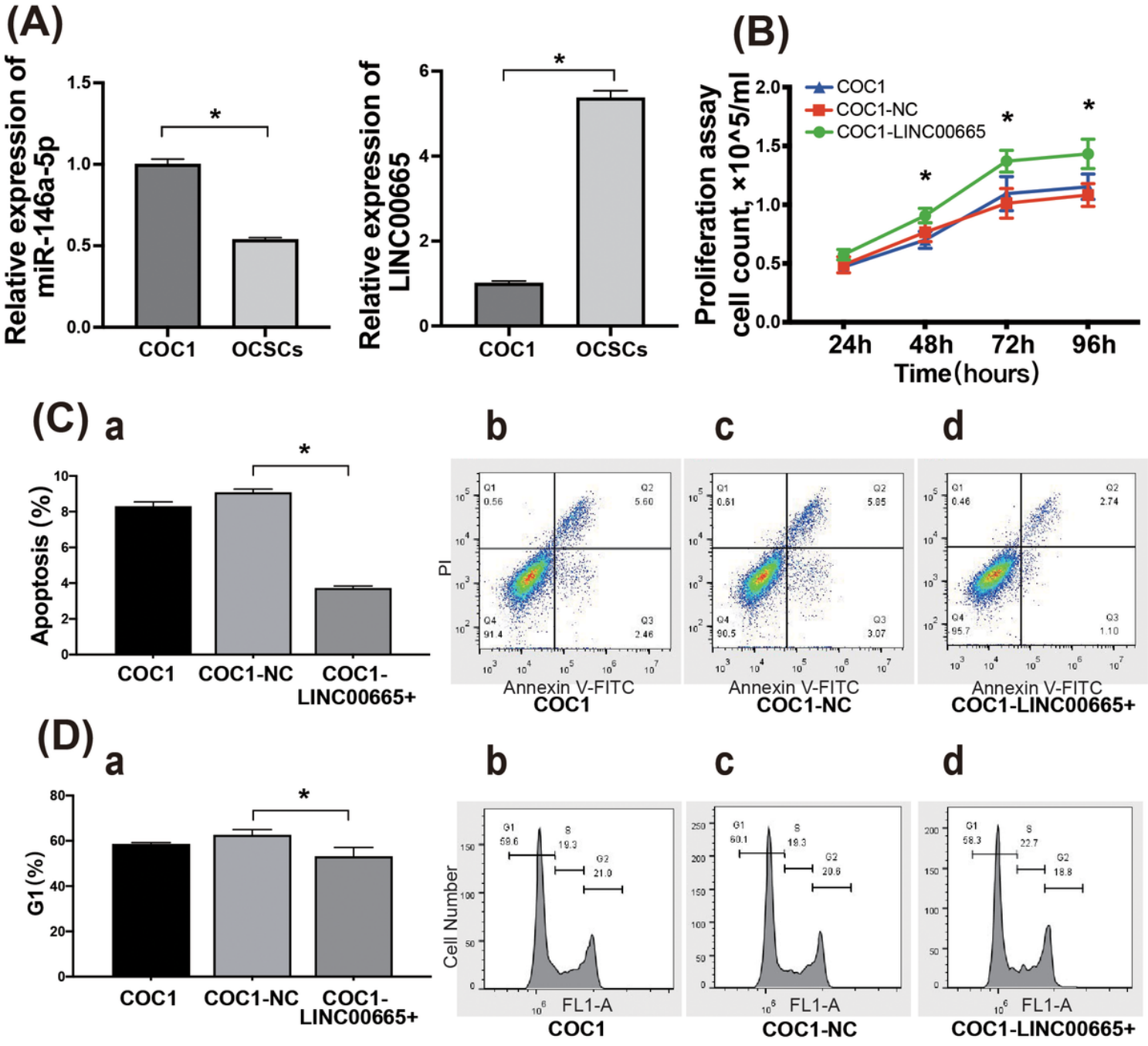

Figure 6

LINC00665 is a lncRNA in the predicted ceRNA network in OCSCs with elevated expression, while miR-146a-5p is a miRNA in the predicted ceRNA network in OCSCs with decreased expression. The differential expression of them in OCSCs and ovarian cancer cells COC1 was verified, and the increased expression of LINC00665 affected the cell proliferation, apoptosis and cell cycle.

(A) the differential expression of miR-146a-5p and LINC00665 between OCSCs and COC1 according to qPCR results, LINC00665 was further overexpressed in COC1, (B) the proliferation ability, (C) percentage

of apoptosis and (D) percentage of G0/G1 cells of LINC00665+ COC1 results were shown. b, COC1, c, COC1-NC, d, COC1-LINC00665+. *indicates P<0.05.

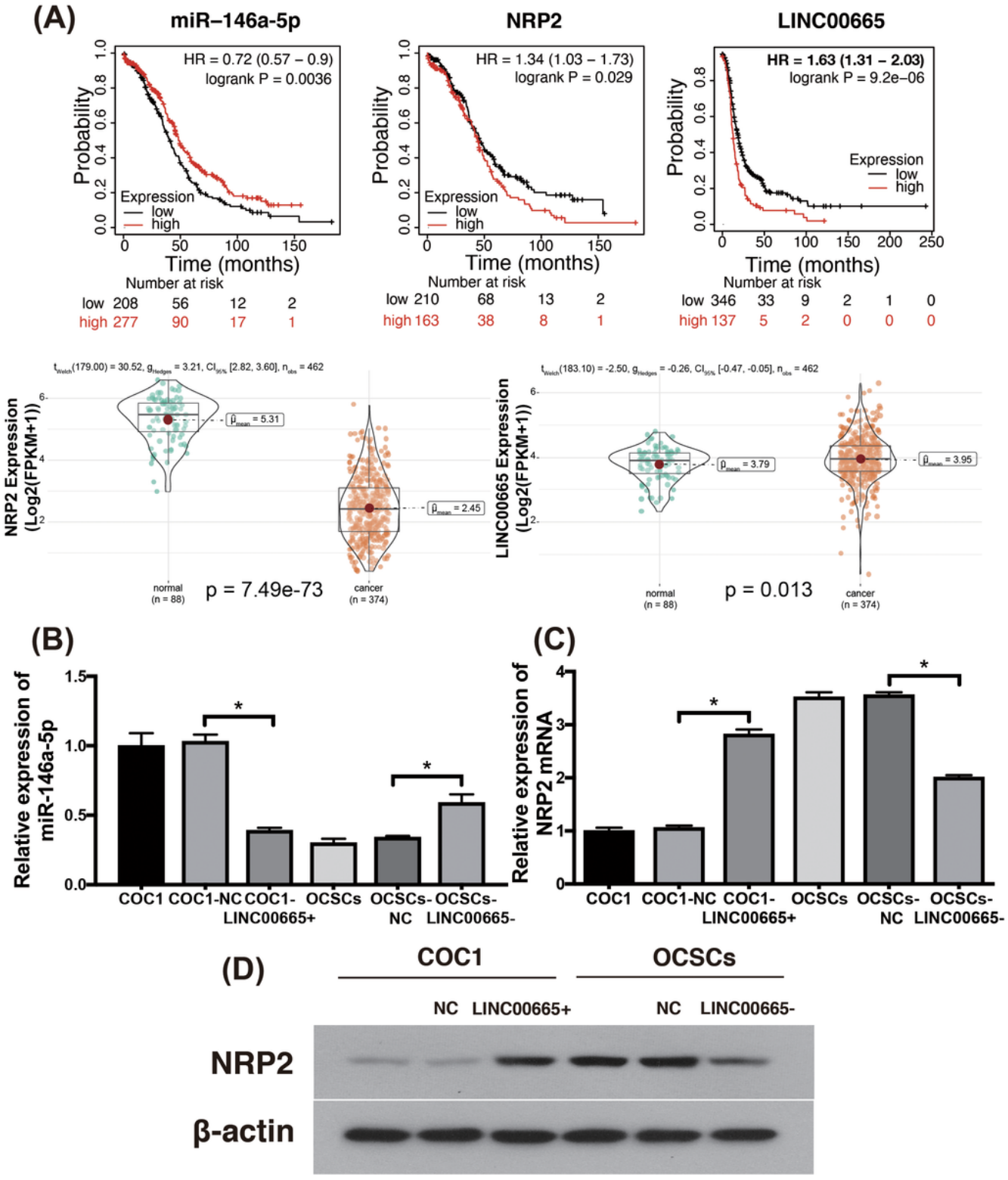

Figure 7

Preliminary validation of the relationship between miR-146a-5p, LINC00665 and NRP2.

(A) Kaplan-Meier (KM) curve analysis of miR-146a-5p, LINC00665 and NRP2 expression with survival probability, and the differentiated expressions of LINC00665 and NRP2 between ovarian cancer and normal samples in OV dataset in TCGA and GTEx calculated by R software (Version 3.6.4). Log2(TPM + 1) was used for log-scale . The exact P-values were marked in each diagram and were all less than 0.05, (B) the differential expression of miR-146a-5p according to qPCR results, LINC00665 was further regulated in COC1 and OCSCs, (C) the differential expression of NRP2 mRNA according to qPCR results, LINC00665 was further regulated in COC1 and OCSCs, (D) the differential expression of NRP2 protein according to qPCR results, LINC00665 was further regulated in COC1 and OCSCs. *indicates P<0.05.

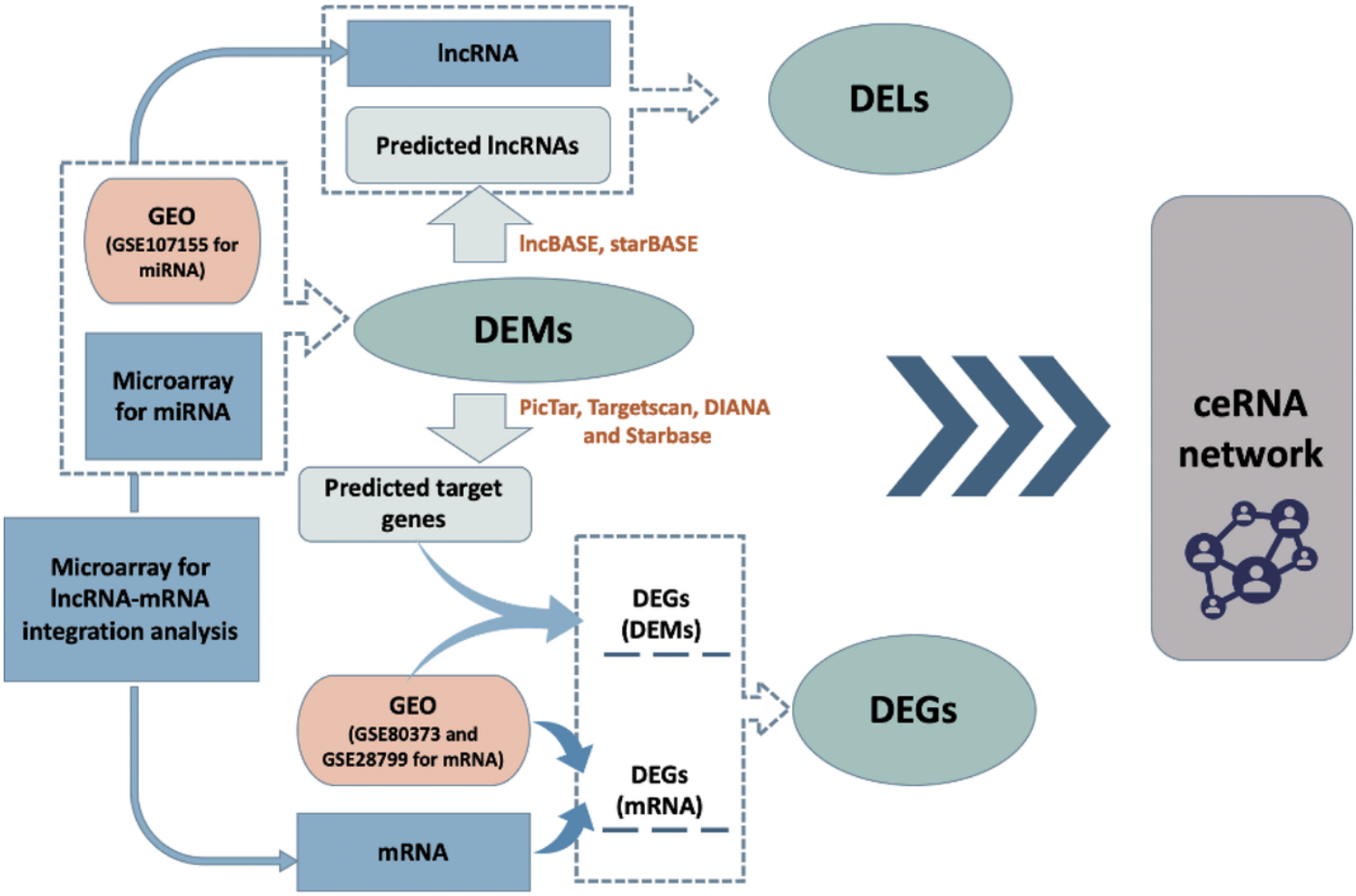

Figure 8

The procedure of the construction of cancer stem cells-associated lncRNA-miRNA-mRNA network for ovarian cancer via microarray and Gene Expression Omnibus database.

Supplementary Files

This is a list of supplementary files associated with this preprint. Click to download.

- Supplementarytablesandfigure.docx
- IFofOCSCsandCOC12.pdf
- IFofOCSCsandCOC1.pdf